Evidence for α clustering in heavy and superheavy nuclei

D. S. Delion*
National Institute of Physics and Nuclear Engineering, POB MG-6, Bucharest-Măgurele, Romania

A. Sandulescu
Center for Advanced Studies in Physics, Calea Victoriei 125, Bucharest, Romania

W. Greiner
Institut für Theoretische Physik, J.W.v.-Goethe Universität, Robert-Mayer-Strasse 8-10, 60325 Frankfurt am Main, Germany
(Received 8 October 2003; published 27 April 2004)

We analyze the α decay between ground states along $N-Z$ chains in deformed heavy and superheavy nuclei, by using the pairing approach. We show that the derivative of the preformation amplitude is practically a constant along any α chain, while that of the outgoing wave function changes exponentially upon the Coulomb parameter. This leads to the breakdown of the continuity equation and therefore to wrong decay widths. The behavior cannot be explained within the standard shell model. We significantly correct this deficiency by considering an α-cluster factor in the preformation amplitude, depending exponentially upon the Coulomb parameter. Thus, four-body correlations, connected with the radial shape of the preformation factor, are directly evidenced by the α-decay systematics. Moreover, this procedure, in principle, fully determines the Q value and is an important development in the α-decay theory. It also allows us to analyze the relative α-clustering structure of the emitter. It turns out that the isotopes close to the region $N>126$ and superheavy nuclei have a stronger clustering behavior. For superheavy region an additional dependence upon the number of interacting α particles is necessary.

DOI: 10.1103/PhysRevC.69.044318 PACS number(s): 21.60.Gx, 23.60.+e

I. INTRODUCTION

The investigation of the α clustering is mainly connected with the binding energy systematics along α lines, i.e., nuclei with the same isospin projection $N-Z$ [1]. The even-odd pair staggering found along these lines can be nicely explained in terms of a "pairing" in the isospin space between proton and neutron pairs, considered as bosons [2]. It turns out that such a "condensate" is more bound when the number of proton and neutron pairs above a double magic nucleus is even, in agreement with the experimental situation.

On the other hand the α-particle energy (Q value), computed as the difference between the binding energies of initial and final systems, is directly connected with the decay width. Therefore the decay width should bring an information on the α-clustering. First of all we mention that the linear dependence between the logarithm of the decay width and the square root of the Q value was explained in the early days of the nuclear physics by Gamow by using a simple picture: a preformed α particle moves in some attractive potential and penetrates the surrounding Coulomb barrier [3]. Several extensive calculations showed that the half-lives of α-particle emitters are well described, by using an equivalent local potential [4–7]. This feature is connected with the important role played by the tail of the wave function inside the Coulomb barrier. The attractive depth and the radius of the repulsive core determines the energy and wave function of the decaying state, understood as a narrow resonance [8]. Due to the large repulsive barrier the WKB approximation of the Coulomb function is a very good approximation [9].

In the last years the investigation of superheavy nuclei by using α-decay chains became a very active field of the nuclear physics. The synthesis of elements with $Z>104$ was suggested by Flerov [10]. It was predicted by using the cold valleys in the potential energy surface for reactions between ^{48}Ca and different heavy targets [11,12]. The existence of such nuclei is strongly connected with the shell closure property of the mean field in this region [13]. Several papers were devoted to the calculation of α-decay half-lives in this region. They used different methods, such as the Viola and Seaborg formula [13], the WKB method describing transitions to rotational states [14], the generalized liquid drop model [15,16], the preformed cluster decay model [17], the empirical Brown formula [18], or the integral kernel method [19]. All of them can be considered as phenomenological approaches, based essentially on the Gamow phenomenological picture.

The R-matrix theory [20,21] makes a step forward and expresses the decay width as a product between the particle preformation probability and the penetration through the barrier. The α-particle preformation probability can be estimated in terms of single-particle states using the Talmi-Moshinski technique [22–24]. Due to the antisymmetrization effects between the α-particle and daughter wave functions the interaction becomes nonlocal in the internal region [25]. The important role played by pairing residual correlations on the preformation factor was evidenced in Ref. [26].

In spite of these theoretical achievements it was shown that the usual shell-model space using $N=6-8$ major shells

*Corresponding author. Fax: 0040-21-4574440. Email address: delion@theor1.theory.nipne.ro

underestimates the experimental decay width by several orders of magnitude [27,28]. This is connected with the exponential decrease of bound single particle wave functions [29]. The inclusion of narrow single particle resonances is not able to cure this deficiency [30–33]. Only the background components in continuum can describe the right order of magnitude of experimental decay widths [34–37].

Anyway, the shell-model estimate of the α-particle preformation factor is not consistent with the decreasing behavior of Q values along any neutron chain [38,39]. In our previous paper [40] we analyzed this feature by treating the α-decaying state as a resonance built in a standard way, namely, by using the matching between logarithmic derivatives of the preformation amplitude and Coulomb function. This is equivalent to the so-called "plateau condition," i.e., the independence of the decay width upon the matching radius. It turns out that this condition is not satisfied along any neutron chain if one uses the standard shell-model estimate for the preformation factor. This happens because the derivative of the penetration factor changes much faster upon the Q values than the internal preformation amplitude. We corrected the slope of the preformation amplitude by changing the harmonic oscillator (ho) parameter of single particle components in continuum. They give the most important contribution in the preformation amplitude. These components are connected with an α-cluster term, not predicted by the standard shell model [41]. Recently a similar idea was used in Ref. [42]. Here the ho parameter, associated with the center of mass (c.m.) α-particle wave function, was used as a variational parameter, describing excited 0^+ states in ^{12}C and ^{16}O.

The aim of this paper is to extend our analysis of the decay widths, by connecting the heavy with superheavy regions along α-like chains. Our purpose is not only to give a correct description of absolute decay widths. We will show that in order to fulfil the plateau condition it is necessary to use an additional α-cluster component, depending upon the Q value. In this way we are able to connect the microscopic clustering properties of α emitters with their binding energies.

The paper is organized according to the following plan. In Sec. II we give all necessary details concerning the penetration of the α particle through a deformed Coulomb barrier and the microscopic calculation of the preformation factor. In Sec. III we first analyze the influence of the relevant parameters upon the decay width. We investigate even-even and favored even-odd α emitters within the standard pairing approach. We then introduce a correcting factor for the α-particle preformation amplitude, in order to achieve self-consistency with the used Q value. We analyze the relative behavior of the additional factor upon the neutron number, giving an important information on the α clustering. Finally we predict half-lives for even-even and even-odd superheavy emitters. In the last section we draw conclusions.

II. THEORETICAL BACKGROUND

We will investigate the α-clusterization process by analyzing the decay widths. The standard procedure to compute the α-decay width within the deformed WKB approach and to estimate the microscopic preformation amplitude was described in several papers, like for instance [34–37]. In this section we will summarize the necessary details.

A. WKB approach for the deformed Coulomb barrier

Let us consider a transition connecting two axially deformed nuclei

$$B(I_i,K_i) \rightarrow A(I_f,K_f) + \alpha(l), \tag{2.1}$$

where (I,K) denotes the total nuclear spin and its projection on the intrinsic axis and l the angular momentum of the emitted α particle.

In general the interaction between the α-particle and the daughter nucleus is given by a nonlocal potential. Beyond the touching radius $R_c=1.2(A_A^{1/3}+4^{1/3})$ Pauli exchange effects diminish, the nuclear potential becomes very small, and the Schrödinger equation governing the cluster motion contains mainly a local component. Due to the fact that only the tail of the preformation factor is important for the decay process in *phenomenological approaches* one defines an equivalent local potential for any distance, i.e.,

$$\left[-\frac{\hbar^2}{2\mu}\Delta + V(\mathbf{r}) \right] \Psi(\mathbf{r}) = E\Psi(\mathbf{r}), \tag{2.2}$$

where $\mathbf{r}=(r,\hat{r})$ denotes the relative distance and $\mu = M_\alpha M_A/(M_\alpha+M_A)$ the reduced mass of the α-daughter system. The equivalent potential is written as follows:

$$V(\mathbf{r}) = V_N(\mathbf{r}), \quad \mathbf{r} \in \text{int}[\mathbf{R}], \quad V_C(\mathbf{r}), \quad \mathbf{r} \in \text{ext}[\mathbf{R}], \tag{2.3}$$

where V_N simulates the internal cluster preformation process, while V_C denotes the Coulomb potential. Here $[\mathbf{R}]$ is the surface between internal and external regions. Thus, we suppose that at a certain surface the α particle is already formed and moves in the Coulomb field of the daughter nucleus. Of course beyond some value R_c the final decay width should not depend on this surface. In Fig. 3 of Ref. [33] by using a microscopic approach we estimated such an equivalent spherical local potential. In the internal region it has a pocketlike shape, but beyond the touching radius $R=R_c\approx 9$ fm it is indeed very close to the Coulomb interaction. This feature is already a signature that the decay width will not depend upon R beyond the touching configuration, as can be seen in Fig. 4 of the same reference.

In a phenomenological approach the decaying state is described as a resonance inside this potential. By expanding the solution in spherical waves

$$\Psi_m(\mathbf{r}) = \sum_l \frac{g_l(r)}{r} Y_{lm}(\hat{r}), \tag{2.4}$$

one finds a resonant state with a given projection m, by matching the internal $g_l^{(\text{int})}(r)$ and external outgoing components $g_l^{(\text{ext})}(r)$ at some radius $r=R$. Thus one determines an eigenstate with complex energy, i.e.,

$$E = E^{(0)} - \frac{i}{2}\Gamma. \tag{2.5}$$

The real part of the energy is adjusted to the experimental Q value by using the depth of the potential as a parameter. For all known α decays the Coulomb barrier is very large and the width Γ is by many orders of magnitude less than the real part. Therefore it is practically impossible to find the imaginary part from the matching condition. But on the other hand the decay width can be derived from the continuity equation as follows:

$$\Gamma = \hbar\nu \sum_l \lim_{r\to\infty} |g_l(r)|^2, \tag{2.6}$$

where ν is the c.m. velocity at infinity.

The external components in a Coulomb field were derived by Fröman within the deformed WKB approach [9]. By introducing them in the above relation one obtains

$$\Gamma = \sum_l \Gamma_l = \hbar\nu \frac{1}{G_0(\chi, kR)^2} \sum_l \left[\sum_{l'} D_{ll'}(R) g_{l'}^{(\mathrm{int})}(R) \right]^2, \tag{2.7}$$

where $G_0(\chi, kR)$ denotes the monopole irregular Coulomb function [43], depending upon the product between the momentum k and matching radius R. Here χ is the Coulomb parameter, defined as twice the Somerfeld parameter

$$\chi = 2\frac{Z_1 Z_2 e^2}{\hbar\nu}. \tag{2.8}$$

By considering that the intrinsic spin projection is conserved $K_i = K_f$ the deformation matrix has the following form:

$$D_{ll'}(R) = \exp\left[-\frac{l(l+1)}{\chi} \sqrt{\frac{\chi}{kR} - 1} \right] \langle I_i K_i; l0 | I_f K_i \rangle K_{ll'}, \tag{2.9}$$

where by bracket we denoted the Clebsch-Gordan coefficient. It turns out that the major effect is given by the quadrupole deformation [35]. In this case the so-called Fröman matrix can be written as follows:

$$K_{ll'} = \int_0^\pi \Theta_{l0}(\theta) e^{BP_2(\cos\theta)} \Theta_{l'0}(\theta) \sin\theta d\theta. \tag{2.10}$$

Here $\Theta_{lm}(\theta)$ are the normalized azimuthal harmonics given by the definition of spherical harmonics, i.e.,

$$Y_{lm}(\theta, \phi) = \Theta_{lm}(\theta) \frac{e^{im\phi}}{\sqrt{2\pi}}, \tag{2.11}$$

and

$$B = \frac{2}{5}\chi\beta_2 \left(2 - \frac{kR}{\chi}\right) \sqrt{\frac{5}{4\pi}\frac{kR}{\chi}\left(1 - \frac{kR}{\chi}\right)}, \tag{2.12}$$

where β_2 is the quadrupole deformation. This result is a very good approximation with respect to the exact coupled channels solution, for quadrupole deformations $|\beta_2| \leqslant 0.3$ [44]. Moreover, our previous calculations [35] showed that 90% of the contribution is given by the monopole component of the internal wave function $g_0^{(\mathrm{int})}(R)$. Therefore the decay width can be estimated by using the following ansatz:

$$\Gamma = \left\{ \hbar\nu \left[\frac{g_0^{(\mathrm{int})}(R)}{G_0(\chi, kR)} \right]^2 \right\} \left\{ \sum_l D_{l0}^2(R) \right\} \equiv \Gamma_0(R) D(R), \tag{2.13}$$

where the function $D(R)$ is given by the sum over angular momentum l. Thus, a very good approximation for the α-decay width from axially deformed nuclei is given by the product between the standard *spherical width*, given by the Thomas formula $\Gamma_0(R)$ [20], and the *deformation factor* $D(R)$. It contains a ratio between the internal and external solutions. The decay width does not depend upon the matching radius R within the local potential approach, because the internal and external wave functions satisfy the same equation and therefore are proportional. This is the so-called plateau condition. The approximation given by Eq. (2.13) satisfy this requirement with a good accuracy.

B. Microscopic α-particle preformation amplitude

The situation becomes different when the value of the internal wave function $g_0^{(\mathrm{int})}(R)$ is given by an independent *microscopic approach*. In this case the internal potential V_N in Eq. (2.3) is replaced by the so-called preformation amplitude. The two-body interaction is defined only in the external region. As we already pointed out in the region beyond R_c the two-body residual interaction, generating the preformation amplitude, is so small that the equivalent local potential practically coincides with V_C. In this case the preformation amplitude and Coulomb wave function do not *a priori* have the same derivatives.

The preformation factor is defined as the amplitude to find α-daughter configuration $\Psi_\alpha \Psi_A$ in initial mother wave function Ψ_B, i.e.,

$$\frac{g_0^{(\mathrm{int})}(R)}{R} \equiv \mathcal{F}_0(R) = \int d\xi_\alpha d\xi_A \Psi_\alpha^*(\xi_\alpha) \Psi_A^*(\xi_A) \Psi_B(\xi_B), \tag{2.14}$$

where the integration is performed over internal coordinates. As the final results below Eq. (2.23) shows it depends only upon R. We neglected the antisymmetrization between the cluster and daughter wave functions, because we will estimate this integral for distances R where the Pauli principle can be neglected.

The structure of a free α particle is very simple. It contains one pair of protons in a singlet state and a similar pair of neutrons. Each particle lies in the ground state 0*s* of an ho well. By recoupling the product of radial wave functions to the relative and c.m. components one obtains

$$e^{-\beta_\alpha r_1^2/2}e^{-\beta_\alpha r_2^2/2}e^{-\beta_\alpha r_3^2/2}e^{-\beta_\alpha r_4^2/2} = e^{-\beta_\alpha(r_\pi^2+r_\nu^2+r_{\pi\nu}^2)/2}e^{-4\beta_\alpha R^2/2} \sim \Psi_\alpha(r_\pi,r_\nu,r_{\pi,\nu})\Psi_{\text{c.m.}}(R). \tag{2.15}$$

Here we introduced Moshinsky relative and c.m. coordinates, respectively,

$$r_\pi = \frac{r_1 - r_2}{\sqrt{2}}, \quad r_\nu = \frac{r_3 - r_4}{\sqrt{2}}, \quad r_{\pi\nu} = \frac{r_1 + r_2 - r_3 - r_4}{2},$$

$$R = \frac{r_1 + r_2 + r_3 + r_4}{4}, \tag{2.16}$$

where r_1, r_2 denote proton and r_3, r_4 neutron coordinates. The size parameter of the intrinsic α-particle potential, determined by electron-scattering experiments, is $\beta_\alpha \approx 0.5\ \text{fm}^{-2}$ [24]. The relative wave function used in Eq. (2.14) contains also proton and neutron singlet spin-wave functions, i.e.,

$$\Psi_\alpha(\xi_\alpha) = \Psi_\alpha(r_\pi,r_\nu,r_{\pi\nu})\chi_0(s_\pi)\chi_0(s_\nu). \tag{2.17}$$

The most important ground state correlations are given by the pairing interaction. We use the Bardeen-Cooper-Schrieffer (BCS) approach for mother and daughter wave functions. In order to estimate the overlap integral (2.14) we expand the mother wave function in terms of sp states, multiplied by the daughter wave function, as follows:

$$\Psi_B = \frac{1}{2}\sum_{j_\pi}\sqrt{j_\pi + \frac{1}{2}}P_{j_\pi}[\psi_{j_\pi} \otimes \psi_{j_\pi}]_0 \sum_{j_\nu}\sqrt{j_\nu + \frac{1}{2}}P_{j_\nu}[\psi_{j_\nu} \otimes \psi_{j_\nu}]_0\Psi_A. \tag{2.18}$$

We use the short-hand index notation $j_\tau \equiv (\tau\epsilon lj)$, where $\tau = \pi, \nu$ denotes isospin, ϵ sp energy, l angular momentum, and j total spin. Otherwise j_τ has the usual meaning of the single particle spin. The expansion coefficients are given in terms of BCS occupation amplitudes as follows:

$$P_{j_\tau} = u_{j_\tau}^{(A)}v_{j_\tau}^{(B)}. \tag{2.19}$$

This expansion contains a pair of proton and one of neutron states, similar to the structure of a free α-particle (2.17). In order to perform the integral (2.14) analytically we expand sp wave functions in the ho basis, i.e.,

$$\psi_{j_\tau m}(\mathbf{r},s) = \sum_{n=0}^{n_{\max}} c_{nj_\tau}\mathcal{R}_{nl}(\beta_0 r^2)[Y_l(\hat{r}) \otimes \chi_{1/2}(s)]_{j_\tau m}, \quad \tau = \pi, \nu. \tag{2.20}$$

The radial ho wave function

$$\mathcal{R}_{nl}(\beta_0 r^2) = \mathcal{N}_{nl}(\beta_0)e^{-\beta_0 r^2/2}r^l L_n^{(l+1/2)}(\beta_0 r^2) \tag{2.21}$$

is defined in terms of the Laguerre polynomial. The sp parameter β_0 is connected with the standard ho parameter by using a scaling factor f_0 as follows:

$$\beta_0 = f_0\beta_N = f_0\frac{M_N\omega}{\hbar} \approx \frac{f_0}{A^{1/3}}, \tag{2.22}$$

where A is the mass number. By performing the recoupling of proton and neutron pairs in Eq. (2.18) to relative and c.m. coordinates the preformation amplitude becomes

$$\mathcal{F}_0(\beta_0, n_{\max}, P_{\min}; R) = e^{-4\beta_0 R^2/2}\sum_N W_N(\beta_0, n_{\max}, P_{\min})\mathcal{N}_{N0}(4\beta_0)L_N^{1/2}(4\beta_0 R^2). \tag{2.23}$$

We stress on the fact that the exponential term is similar to the c.m. α-particle wave function (2.15), but it depends upon the single particle ho parameter β_0. We will show that this term is directly connected with the plateau condition and gives the main clustering feature of the α-decay process. The expansion coefficients are given in terms of recoupling Talmi-Moshinsky brackets as follows:

$$W_N(\beta_0, n_{\max}, P_{\min}) = 8\sum_{nN_\pi N_\nu}\langle n0N0;0|N_\pi 0N_\nu 0;0\rangle\mathcal{I}_{n0}^{(\beta_0,\beta_\alpha)}G_{N_\pi}G_{N_\nu}. \tag{2.24}$$

The quantities $\mathcal{I}_{n0}^{(\beta_0,\beta_\alpha)}$ are overlap integrals between radial ho functions, i.e.,

$$\mathcal{I}_{n0}^{(\beta_0,\beta_\alpha)} = \int_0^\infty \mathcal{R}_{n0}(\beta_0 r^2)\mathcal{R}_{00}(\beta_\alpha r^2)r^2 dr. \tag{2.25}$$

The proton coefficients $G_{N\pi}$ are given by the following relation:

$$G_{N_\pi} = \sum_{ljn_\pi}\sum_{n_1 n_2=0}^{n_{\max}} B_\pi(n_1 l j n_2 l j) \times \left\langle (ll)0\left(\frac{1}{2}\frac{1}{2}\right)0;0\middle|\left(l\frac{1}{2}\right)j\left(l\frac{1}{2}\right)j;0\right\rangle \times \langle n0N_\pi 0;0|n_1 l;n_2 l;0\rangle\mathcal{I}_{n_\pi 0}^{(\beta_0,\beta_\alpha)}. \tag{2.26}$$

The first bracket denotes $jj-LS$ recoupling coefficient, while the second one Talmi-Moshinsky symbol. B coefficient is a sum over all sp states with given spherical quantum numbers, i.e.,

$$B_\pi(n_1 l j n_2 l j) = \sum_{P_{j_\pi} \geqslant P_{\min}}\sqrt{j_\pi + \frac{1}{2}}P_{j_\pi}c_{n_1 j_\pi}c_{n_2 j_\pi}. \tag{2.27}$$

Therefore we consider in our sp basis only those states with P_τ larger than the minimal value $P_{\min}$, taken as a parameter.

One obtains a similar relation for G_{N_ν}.

III. ANALYSIS OF α-DECAY CHAINS

The natural way to analyze α decays is along the so-called α chains, connecting nuclei with the same isospin projection $I = N - Z$. A systematics of α-decay Q values along these lines was for the first time performed in Ref. [1]. Here it was

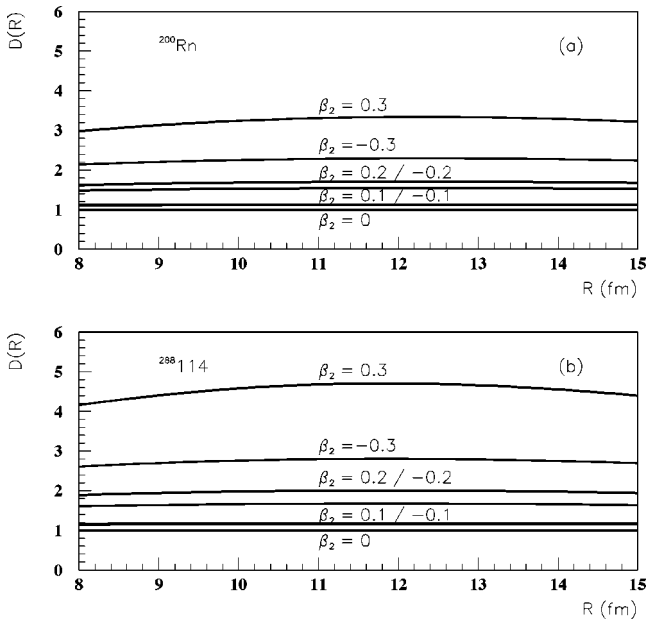

FIG. 1. (a) The dependence of the deformation factor $D(R)$ defined by Eq. (2.13) upon the matching radius, for different quadrupole deformations. The decay process is $^{200}\mathrm{Rn}\rightarrow{}^{196}\mathrm{Po}+\alpha$. (b) The same as in (a) but for the decay process $^{288}114\rightarrow{}^{284}112+\alpha$.

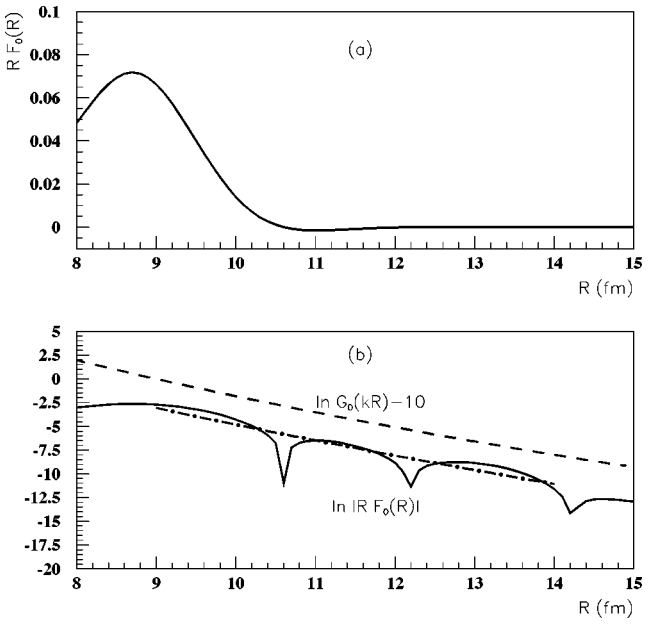

FIG. 2. (a) The preformation amplitude $R\mathcal{F}_0(R)$ vs the matching radius for the decay process $^{200}\mathrm{Rn}\rightarrow{}^{196}\mathrm{Po}+\alpha$. (b) The natural logarithm of the modulus of the preformation amplitude (solid line), the natural logarithm of the irregular Coulomb function $G_0(\chi,kR)$ (dashed line), and the linear fit of the solid curve (dot-dashed line) vs the matching radius.

evidenced a dependence upon I and I^2 and also upon the number of α-clusters $N_\alpha=(N-N_0)/2$ and N_α^2, where N_0 is the magic neutron number.

The superheavy nuclei are detected using α decays along these paths. One of our goals is to give reliable predictions for half-lives along superheavy chains with $Z>102$, by connecting them with similar chains in heavy nuclei with $82<Z<100$. At the same time we are interested in obtaining the best possible consistency (plateau condition) between the microscopic preformation amplitude and the penetration through the barrier, i.e., the Q value. This will allow us to analyze the relative clustering behavior of α emitters.

A. The parameters of the model

In order to understand the structure of the decay width it is necessary a careful analysis of all significant parameters. Let us first analyze the relevant parameters for the barrier penetration. They concern the irregular Coulomb function $G_0(\chi,kR)$ and the deformation factor $D(R)$ in Eq. (2.13). It is already well known that the barrier penetration is sensitive with respect to the following two parameters:

(1) χ: the Coulomb parameter defined by Eq. (2.8).

(2) β_2: the quadrupole deformation in the Fröman matrix (2.10).

The most important ingredient, governing the penetrability of the α particle through the barrier, is the Coulomb parameter χ. The irregular Coulomb function $G_0(\chi,kR)$ depends exponentially on it. For all known α decays its WKB estimate (Gamow function)

$$G_0(\chi,kR)=(ctg\ \alpha)^{1/2}\ e^{\chi(\alpha-\sin\ \alpha\ \cos\ \alpha)},$$

$$\cos^2\alpha=\frac{kR}{\chi}=\frac{R}{R_0},\quad R_0=\frac{Z_1Z_2e^2}{E},\tag{3.1}$$

gives an error less than 1% with respect to the exact function. It explains the linear dependence between the logarithm of the decay widths and $\sqrt{E}$.

The decay width has also an exponential dependence upon the quadrupole deformation, given by Eqs. (2.10) and (2.12). In order to clarify the role of the barrier deformation we plotted in Fig. 1 the function $D(R)$ in Eq. (2.13) versus the c.m. radius R. We analyzed nuclei at the extremes of the considered interval, namely, ^{200}Rn, (a) and ^{288}114 (b). We considered a typical range of quadrupole deformations for the mother nucleus, i.e., $-0.3<\beta_2<0.3$. In all cases $D(R)$ practically does not depend upon the radius. On the other hand the largest correction gives a factor of 3 for heavy nuclei and a factor of 5 in superheavy ones. From this analysis it becomes clear that the small difference in deformations for mother and daughter nuclei gives practically no correction.

Let us now analyze the important parameters for the preformation factor $g_0^{(\mathrm{int})}(R)=R\mathcal{F}_0(R)$ in Eq. (2.13). The microscopic structure of the preformation amplitude is given by Eq. (2.23). It is very collective and therefore the transitions between ground states are not sensitive to the mean-field parameters. Thus, in our analysis we used the universal parametrization of the Woods-Saxon potential [45]. We solved the BCS equations for the mother and daughter nuclei, but the product af amplitudes $u^{(A)}v^{(B)}$ in Eq. (2.19) differ by 2% from $u^{(B)}v^{(B)}$. Thus, we considered the gap parameter estimated by $\Delta_\tau=12/\sqrt{A_B}$ [46], where A_B is the mass number of

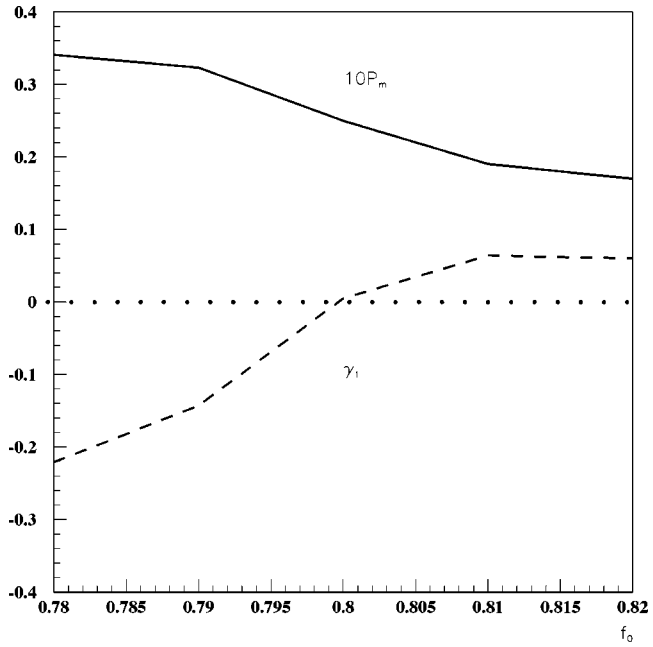

FIG. 3. The parameter $P_{\min}$ multiplied by 10 (solid line) and the slope coefficient γ_1 (dashed line) for $\gamma_0=0$ in Eq. (3.3) vs the ho size parameter f_0 defined by Eq. (2.22). The decay process is $^{200}\mathrm{Rn}\rightarrow{}^{196}\mathrm{Po}+\alpha$.

the mother nucleus, because again the preformation amplitude is not sensitive upon its local fluctuation.

It turns out that the approach is very sensitive with respect to the following three parameters, entering the preformation amplitude.

(1) $n_{\max}$: the maximal sp radial quantum number defined by Eq. (2.20).

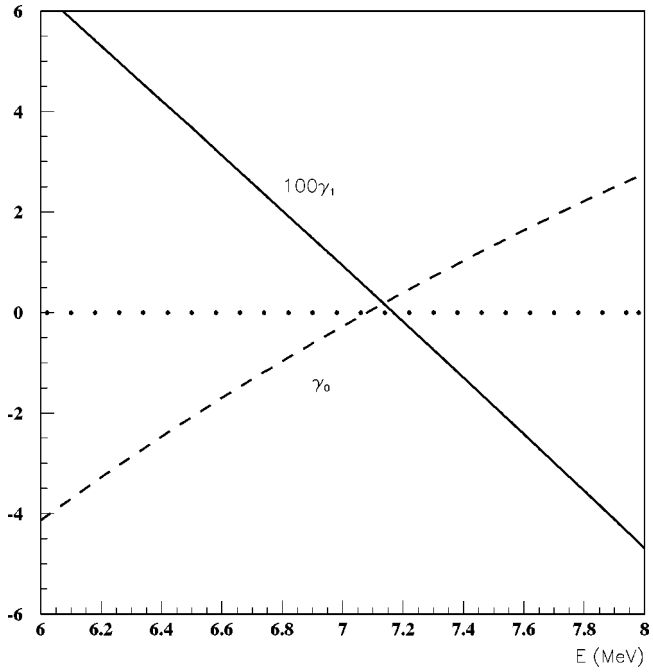

FIG. 4. The slope parameter $100\gamma_1$ (solid line) and the ratio parameter γ_0 (dashed line) in (3.3) vs the α-particle energy for $^{200}\mathrm{Rn}\rightarrow{}^{196}\mathrm{Po}+\alpha$.

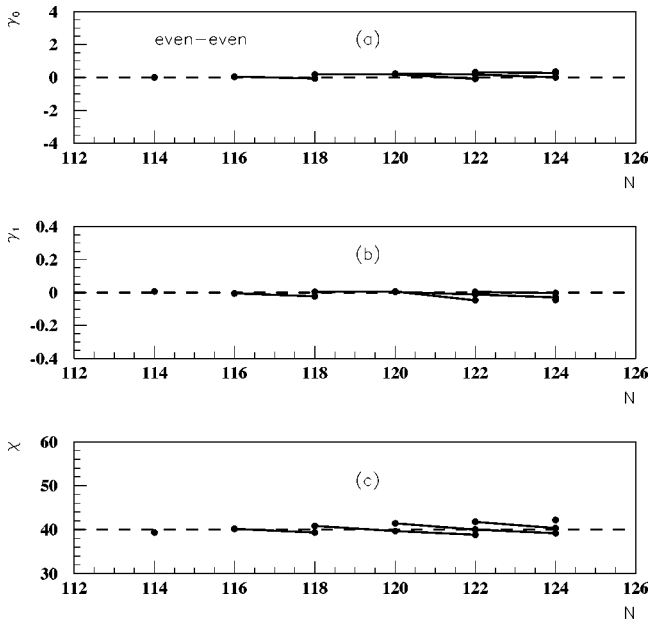

FIG. 5. (a) The ratio parameter γ_0, defined by Eq. (3.3), vs the neutron number for $f_0=0.8, P_{\min}=0.025$ and different even-even α-chains in Table I. (b) The slope parameter γ_1, defined by Eq. (3.3), vs the neutron number and different even-even α-chains in Table I. (c) The Coulomb parameter χ, defined by Eq. (2.8), vs the neutron number and different even-even α-chains in Table I.

(2) β_0: the sp ho parameter, depending upon f_0 defined by Eq. (2.22).

(3) The amount of spherical configurations taken in the BCS calculation, given by $P_{\min}$ in Eq. (2.27), defined as the minimal considered P_τ (2.19).

Let us first analyze the influence of the maximal radial quantum number $n_{\max}$, defining the radial extension of the wave function. For bound states one has $n_{\max}\leqslant 4$. For states in continuum it increases with the sp energy ϵ. This is a very important parameter because the preformation factor should be properly described at large distances, where the states in continuum play an important role. The ideal procedure is to discretize the positive sp spectrum and to find the wave functions by a direct numerical integration. Then the expansion coefficients c_n in Eq. (2.20) can be found by a fitting procedure. In this way the amount of states for each combination l,j will be very large.

Anyway, we are interested in the effective description of the decay width. Namely, if we are able to obtain the value of the decay width for a given nucleus, the other transitions are described by using the same parametrization of the sp spectrum. Thus, we preferred an effective description of the continuum, by using the direct diagonalization method to find the expansion coefficients c_n in the ho basis. It turns out that beyond $n_{\max}=9$ the results saturate if one considers in the BCS basis sp states with $P\geqslant P_{\min}=0.02$. Therefore we considered in our further calculations the value $n_{\max}=9$.

We improved the description of the continuum by choosing a sp scale parameter $f_0<1$ in Eq. (2.22). This is similar to our previous procedure of Ref. ([37]), where we used two ho parameters, one connected with the bound sp spectrum and another one (smaller) with the continuum. A smaller ho

TABLE I. Even-even (left side) and even-odd (right side) α-decay chains in the region $Z>82$, $82<N<126$. In the first column of each table is given the isospin projection $I=N-Z$. In the next columns are given the initial neutron and proton numbers, the number of states/chain and the reference.

I	N_1	Z_1	No	Ref.	I	N_1	Z_1	No	Ref.
28	114	86	1	[7]	27	113	86	1	[7]
30	116	86	2	[7]	29	115	86	2	[7]
32	118	86	3	[7]	31	117	86	3	[7]
34	120	86	3	[7]	33	119	86	3	[7]
36	122	86	2	[7]	35	121	86	2	[7]
38	124	86	1	[7]	37	123	86	1	[7]

parameter corresponds to a larger density of the sp spectrum. We simplified this approach by using only one parameter, because practically only sp states above the Fermi level contribute in the decay width. Actually we found out that the sp states below the Fermi surface give a contribution about few percents in the decay width. Thus, by using a smaller ho parameter the sp wave function, and therefore the preformation amplitude, becomes flatter and it is better described at large distances.

This parameter is not independent from $P_{\min}$. It turns out that the common choice of f_0 and $P_{\min}$ ensures not only the right order of magnitude for the decay width, but also the above mentioned continuity of the derivative. As we already pointed out in the preceding section the continuity of derivatives between the internal preformation factor $g_0^{(\mathrm{int})}(R)=R\mathcal{F}_0(R)$ and the external Coulomb function $G_0(\chi,R)$ is not a trivial condition. This is a necessary condition, because if their slopes are equal the two functions are proportional and according to Eq. (2.13) the decay width does not depend upon R [$D(R)$ is practically a constant]. Obviously this requirement is equivalent to the standard logarithmic derivative condition in finding a resonant state.

In Fig. 2(a) we plotted the preformation amplitude $g_0^{(\mathrm{int})}(R)=R\mathcal{F}_0(R)$ as a function of the radius R for the decay process

$$^{200}\mathrm{Rn} \rightarrow {}^{196}\mathrm{Po} + \alpha. \tag{3.2}$$

It is peaked in the internal region. As it was shown in Ref. [33] a wave function of such a shape is generated by an equivalent pocketlike local potential in the internal region. Its tail in the external region, beyond R_c, corresponds practically to a Coulomb interaction, as in Fig. 3 of Ref. [33]. The asymptotic behavior in this region is exponential, similar to the Coulomb function (3.1), and this feature can be better analyzed in the logarithmic scale. In Fig. 2(b) by a solid line we plotted $\ln|R\mathcal{F}_0(R)|$ and by a dashed line $\ln G_0(\chi,kR) - 10$. By a dot-dashed line we also give the linear fit of the preformation amplitude in the interval over 5 fm beyond the touching radius. One sees that it is parallel with the logarithm of the Coulomb function, their difference is a constant, and indeed the plateau condition is fulfilled. Therefore the coefficients of the linear fit

$$\log_{10}\left[\frac{\Gamma(R)}{\Gamma_{\exp}}\right] = \gamma_0 + \gamma_1 R, \tag{3.3}$$

should vanish, i.e. $\gamma_0=\gamma_1=0$, in order to have a proper description of the decay width. It turns out that they are very sensitive to the size parameter f_0 and $P_{\min}$. In Fig. 3 we plotted by a solid line the value of 10 $P_{\min}$ versus f_0, for which we obtained $\gamma_0=0$. By a dashed line it is given the value of the slope γ_1 for the same condition. One can see that one obtains $\gamma_0=\gamma_1=0$ for $f_0=0.8$ and $P_{\min}=0.025$. This corresponds to about 50 spherical configurations in Eq. (2.24), and sp spectra are bound by the following limits $\max|\epsilon_\pi|\approx 15$ MeV, $\max|\epsilon_\upsilon|\approx 5$ MeV.

In other words we can, in principle, find the Coulomb parameter χ by solving the equation

$$\gamma_1(\chi) = 0, \tag{3.4}$$

for given parameters $n_{\max},\beta_0,P_{\min}$ and in this way *to pre-*

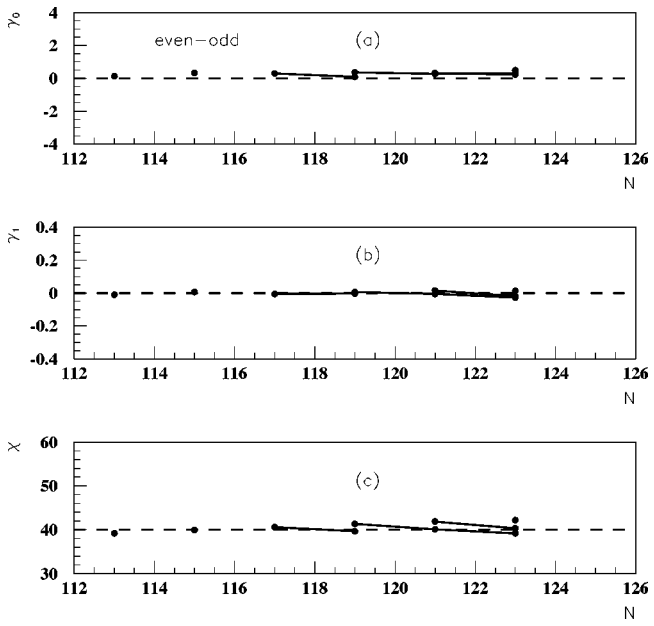

FIG. 6. (a) The same as in Fig. 5(a), but for different even-odd α-chains in Table I. (b) The same as in Fig. 5(b), but for different even-odd α-chains in Table I. (c) The same as in Fig. 5(c), but for different even-odd α-chains in Table I.

TABLE II. Even-even (left side) and even-odd (right side) α-decay chains in the region $Z>82$, $N>126$. The quantities are the same as in Table I.

I	N_1	Z_1	No	Ref.	I	N_1	Z_1	No	Ref.
38	130	92	1	[7]	39	131	92	1	[7]
40	130	90	2	[7]	41	131	90	2	[7]
42	130	88	3	[7]	43	131	88	5	[7]
44	130	86	6	[7]	45	131	86	7	[7]
46	132	86	8	[7]	47	133	86	8	[7]
48	134	86	12	[7]	49	139	90	11	[7,49]
50	136	86	9	[7]	51	143	92	8	[7]
52	142	90	7	[7]	53	147	94	10	[7,50]
54	146	92	5	[7]	55	151	96	4	[7]
56	150	94	4	[7]	57	155	98	2	[7]
58	154	94	2	[7]	59	173	114	1	[7]
60	172	112	3	[48]	61	175	114	3	[51]

dict Q value independently, based only on the microscopic factor. This equation involves only the theoretical estimate of the decay width, because it is independent on the constant $\Gamma_{\exp}$. In order to analyze the sensitivity of the slope parameter γ_1 upon the Q value we plotted in Fig. 4 their dependence. One can see that it is necessary to solve the above Eq. (3.4) with an error $|\gamma_1| \leqslant 0.02$, to achieve a precision of 500 keV.

B. α chains for $Z>82$, $82<N<126$

We used the values of the parameters determined above, $n_{\max}=9$, $f_0=0.8$ and $P_{\min}=0.025$, in order to analyze other α decays. A correct theoretical description should give small fluctuations for γ_0 and γ_1, if the α clustering is entirely described within this approach. Indeed, this is the case for the region $Z>82$, $82<N<126$. The above analyzed decay (3.2) belongs to this region, containing six even-even α chains, described in the left side of the Table I. Here we give the values of $I=N-Z$, the starting values N_1 and Z_1 and the number of states/chain. In the last column we give the reference for the experimental decay widths and Q values. In all cases $I_i=I_f=0$ in Eq. (2.9). The quadrupole deformation parameters are taken from Ref. [47].

In Figs. 5(a) and 5(b) we plotted the parameters γ_0, γ_1 depending upon the neutron number. One can see that indeed their values are very close to zero. The decay widths are reproduced within a factor of 2. We point out in advance that the small decrease of parameters along considered α chains is correlated with a similar behavior of the Coulomb parameter χ in Fig. 5(c).

The situation is similar for the favored α decays from even-odd nuclei. We analyzed six even-odd α chains with $I_i=I_f$, described in right side of the Table I. In Figs. 6(a)–6(c) we can see the same behavior as in Figs. 5(a)–5(c).

In conclusion the pairing description of α decays in this region seems to be successful concerning both the ratio to the experimental width and the continuity of derivatives. Moreover, we conclude that the α clustering is constant for all considered emitters.

C. α chains for $Z>82$, $N>126$

The situation completely changes in the region above the magic neutron number $N>126$. We investigated 12 even-even α-chains. They are described in the left side of the Table II.

In Fig. 7(a) we plotted the parameter γ_0 versus the neutron number along these chains. From this figure it is rather difficult to follow each chain from the lowest neutron number N_1. Anyway our purpose is not to identify "who is who," but to show that the general behavior of this parameter is very similar for any considered α chain. One can see that the experimental decay widths are reproduced worse than in the previous interval, namely, the quantity $\gamma_0 \approx \log_{10}(\Gamma/\Gamma_{exp})$ has a variation of one order of magnitude around $\gamma_0=0$. This performance can be considered satisfactory for a microscopic model. But at the same time the description of the slope γ_1, given in Fig. 7(b), is by far not satisfactory.

The situation is similar for favored α decays from even-odd nuclei. These chains are described in the right side of the Table II for 12 even-odd α-chains.

In Figs. 8(a) and 8(b) we give the values of the parameters γ_0 and γ_1, respectively, depending upon the neutron number. Again the ratio parameter γ_0 has a variation of one order of magnitude around $\gamma_0=0$ and the variation of the slope γ_1 is very strong. As expected γ_0 has a stronger variation around the semimagic neutron numbers $N=152$ and $N=162$. We partially explain large fluctuations of the ratio parameter γ_0 in the superheavy region by relative large experimental errors.

The reason for the variation of the slope parameter γ_1 is the relative strong dependence of the Coulomb parameter χ upon the neutron number along α chains. In Fig. 9(a) we give the values of this parameter for the even-even chains and in Fig. 9(b) for even-odd chains. The variation of the slope parameter γ_1 for even-even nuclei in Fig. 7(b) is in an obvious correlation with the Coulomb parameter χ in Fig. 9(a). The same happens for even-odd emitters, namely, the slope parameter in Fig. 8(b) is similar to the Coulomb parameter in Fig. 9(b).

It is well known that the derivative of the irregular Coulomb function strongly changes with respect to the parameter

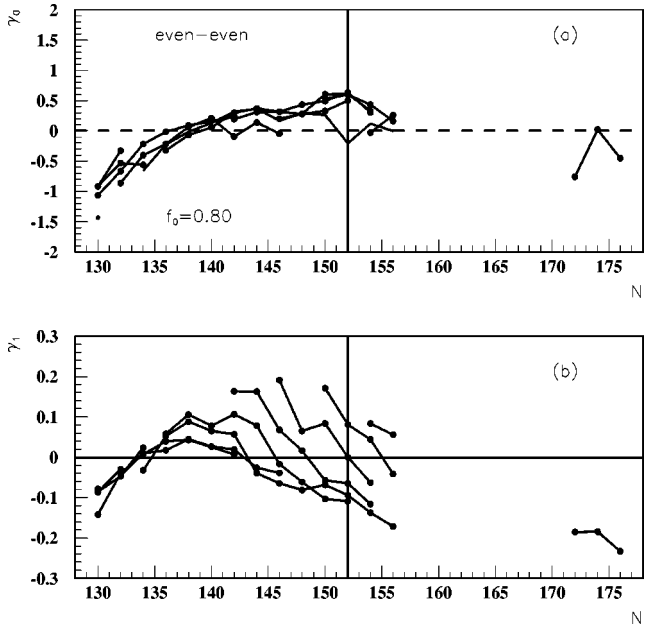

FIG. 7. (a) The parameter γ_0 vs the neutron number for different even-even α-chains in Table II. The preformation parameters are $f_0=0.8$, $P_{\min}=0.025$. (b) The same as in (a), but for the slope parameter γ_1.

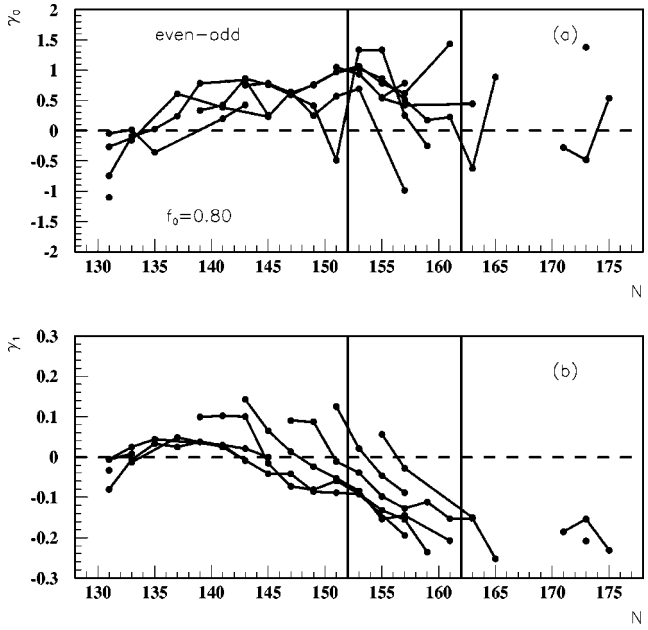

FIG. 8. (a) The parameter γ_0 vs the neutron number for different even-odd α-chains in Table II. The preformation parameters are $f_0=0.8$, $P_{\min}=0.025$. (b) The same as in (a), but for the slope parameter γ_1.

χ. Therefore the derivative of the microscopic preformation amplitude changes along α chains much slower in comparison with that of the Coulomb function. Thus, the microscopic description within the pairing model is not consistent in this region. The discontinuity of the derivative has a profound consequence, namely the continuity equation is not anymore satisfied, because the probability current has a jump.

D. Corrected preformation amplitude

In spite of the fact that this method is used for many years the obvious inconsistency of the shell model, in particular, of the pairing α-decay approach, was only recently stressed in Ref. [40].

At the first sight it seems that this effect could be a consequence of the fact that we considered only the Coulomb interaction in the external region and neglected the equivalent local potential produced by the microscopic preformation factor. Anyway a simple estimate, similar to that in Ref. [33] shows that first of all this correction is very small. On the second hand from our analysis along α chains it turns out that this effect is proportional to the Coulomb parameter χ. The variation due to the potential generated by the microscopic part along any isotope chain is by far not able to follow the trend given by the Coulomb parameter.

Our estimate shows that the linear correlation coefficient between γ_1 and χ is larger than 0.7. This allows us to introduce a supplementary, but universal, correcting procedure for the preformation factor. Thus, let us define a variable size parameter f by a similar to Eq. (2.22) relation, namely,

$$\beta = f\beta_N. \tag{3.5}$$

The parameter χ enters in the exponent of the Coulomb function (3.1). This fact suggests a similar correction of the preformation factor, i.e.,

$$\overline{\mathcal{F}}_0(\beta,\beta_m,n_{\max},P_{\min};R) = e^{-4\beta R^2/2}\sum_N W_N(\beta_m,n_{\max},P_{\min})\mathcal{N}_{N0}(4\beta_m)L_{N0}^{(1/2)}(4\beta_m R^2). \tag{3.6}$$

Therefore we decouple the ho parameter, entering the clusterlike exponential factor, from the fixed parameter sp ho parameter β_m. We suppose a linear dependence of the size parameter f upon the Coulomb parameter

$$\beta-\beta_m=(f-f_m)\beta_N=f_1(\chi-\chi_m)\beta_N. \tag{3.7}$$

The above relation (3.6) can be written as follows:

$$\begin{aligned}\overline{\mathcal{F}}_0(\beta,\beta_m,n_{\max},P_{\min};R) &= e^{-4(\beta-\beta_m)R^2/2}\mathcal{F}_0(\beta_m,n_{\max},P_{\min};R)\\ &= \mathcal{F}_0(\beta-\beta_m,0,0;R)\mathcal{F}_0(\beta_m,n_{\max},P_{\min};R),\end{aligned} \tag{3.8}$$

i.e., the usual preformation amplitude is multiplied by a cluster preformation amplitude with $n_{\max}=0$. Thus, one has to multiply the right-hand side of the expansion (2.23) by this factor.

Our calculations showed that indeed, this is the best choice for the slope correction of the preformation amplitude. If one uses a variable ho parameter for the second factor in the above relation one always obtains a linear decreasing trend of the slope parameter γ_1 along any α chain. This is a strong argument in favor of the α-clustering nature of this correction.

The energy of the emitted particle can be splitted into two components, a pure shell model plus a cluster part, i.e.,

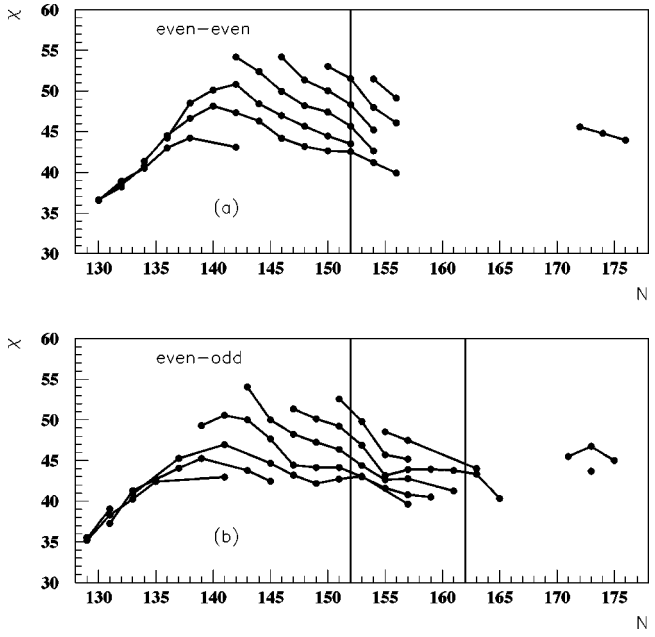

FIG. 9. (a) The Coulomb parameter χ vs the neutron number for different even-even α-chains in Table II. (b) The Coulomb parameter χ vs the neutron number for different even-odd α-chains in Table II.

$$E = E_{\beta_m} + E_{\beta-\beta_m}. \tag{3.9}$$

Therefore the Q-value contains a smooth part and a fluctuation, given by four-body correlations not included in the pairing model. This representation is somehow similar to the standard Strutinsky procedure to split the binding energy into a smooth liquid drop term plus a shell-model fluctuation [52], but of course the two terms in our case have different meanings.

First of all we tried to maintain our previous parametrization for $N<126$, i.e., $f_m=0.8$, $\chi_m=0.40$, by looking for the best slope f_1 in Eq. (3.7). In this way the first region would be described with the same set of parameters, because the

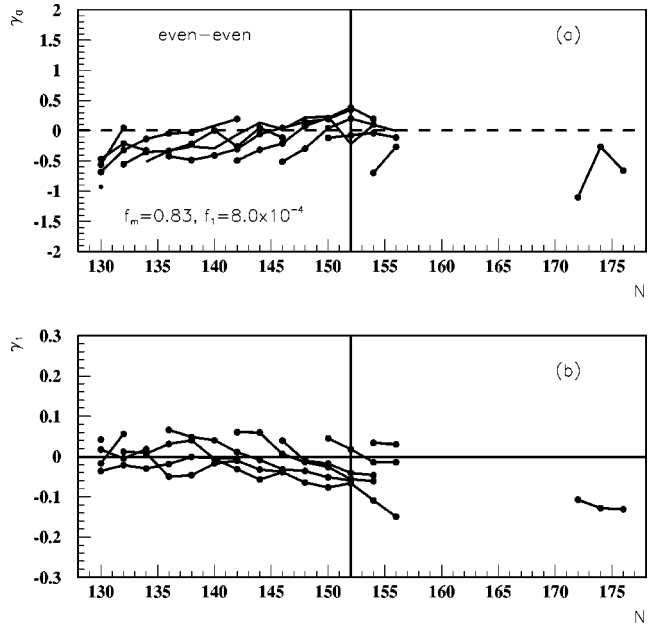

FIG. 10. (a) The parameter γ_0 vs the neutron number for different even-even α-chains in Table II. The preformation parameters are $f_m=0.83$, $f_1=8.0\ 10^{-4}$, $P_{min}=0.025$. (b) The same as in (a), but for the slope parameter γ_1.

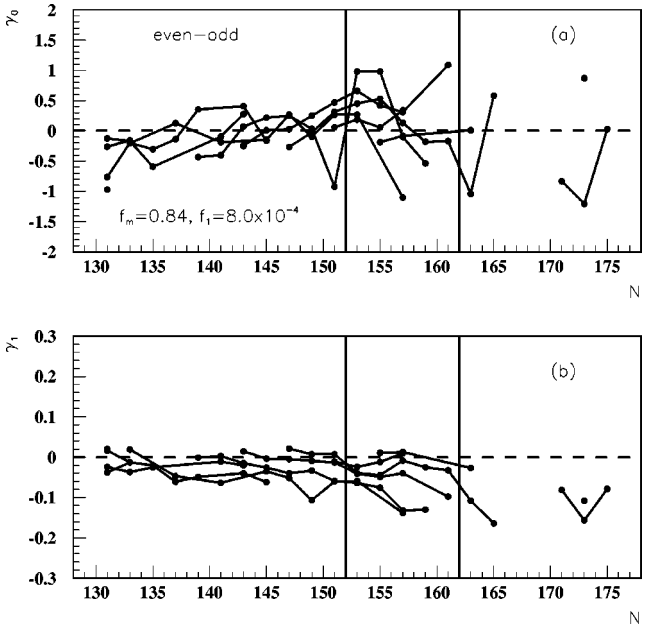

FIG. 11. (a) The parameter γ_0 vs the neutron number for different even-odd α-chains in Table II. The preformation parameters are $f_m=0.84$, $f_1=8.0\ 10^{-4}$, $P_{\min}=0.025$. (b) The same as in (a), but for the slope parameter γ_1.

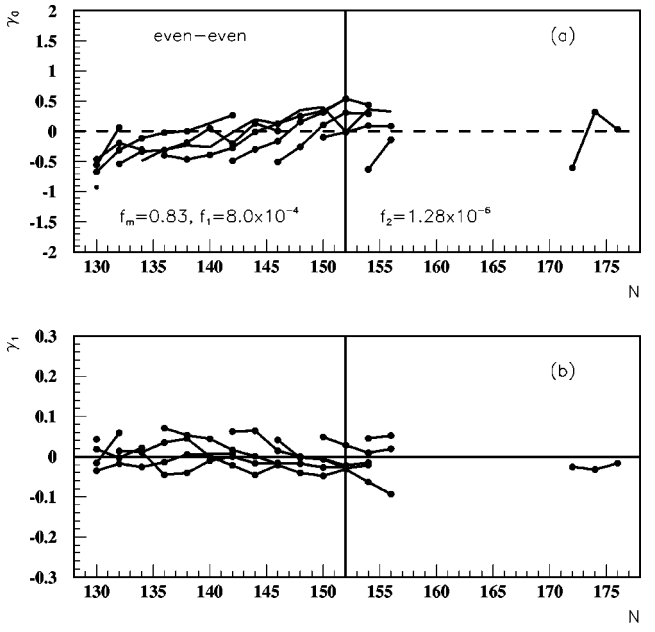

FIG. 12. (a) The parameter γ_0 vs the neutron number for different even-even α-chains in Table II. The preformation parameters are $f_m=0.83$, $f_1=8.0\ 10^{-4}$, $f_2=1.28\ 10^{-6}$, $P_{\min}=0.025$. (b) The same as in (a), but for the slope parameter γ_1.

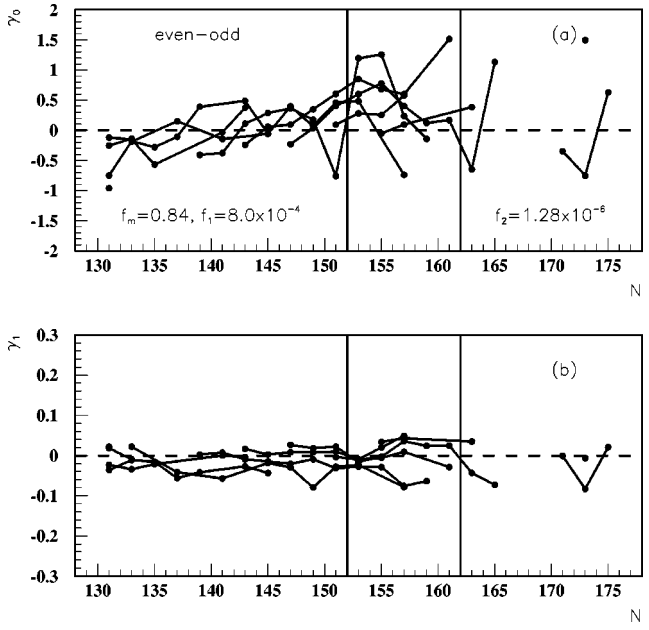

FIG. 13. (a) The parameter γ_0 vs the neutron number for different even-odd α-chains in Table II. The preformation parameters are $f_m=0.84$, $f_1=8.0\ 10^{-4}$, $f_2=1.28\ 10^{-6}$, $P_{\min}=0.025$. (b) The same as in (a), but for the slope parameter γ_1.

Coulomb parameter $\chi\approx 0.40$ for all decays, as can be seen from Figs. 5(c) and 6(c) and we will obtain practically the same values as in Figs. 5(a), 5(b), 6(a), and 6(b). By using this parametrization the ratio parameter indeed improves, becoming closer to a vanishing value for all decays in the region $N>126$, but the description of the slope parameter is still unsatisfactory.

Therefore we chose a different strategy connected with the maximal value of the ratio parameter γ_0. As we will show later this choice has a physical meaning connected with the α-clustering picture. In this way the parametrization in the region $82<N<126$ becomes different with respect to the other one, but at the same time it is common for all α-decaying nuclei with $N>126$, including the superheavy ones. This choice is not a drawback, but it fits the spirit of the Nilsson shell-model parametrization. We remark from Figs. 7(a) and 9(a) that the maximal value of the ratio parameter γ_0 corresponds to a maximal value of the Coulomb parameter. Let us point out that by using a constant ho parameter with the size parameter $f_m=0.83$ for all analyzed even-even emitters the Figs. 7(a) and 7(b) are pushed down and one obtains for the maximal value of the ratio parameter $\gamma_0(\max)=0$. At this point the α clustering is described entirely by the pairing correlations. As we pointed out it roughly corresponds to the maximal value of the Coulomb parameter, namely, $\chi_m=55$. In this way for other decays the α clustering process increases by decreasing the Coulomb parameter, because the ho parameter β in Eq. (3.7) is smaller and therefore the tail of the preformation factor increases. *This is consistent with the physical meaning of the α-clustering process, because a smaller Coulomb parameter correspond to a larger Q-value and consequently to a larger emission probability*.

From Figs. 9(a) and 9(b) we can see that the α clustering is enhanced in the region above $N=126$ and in superheavy nuclei. This is agreement with several calculations pointing out on a very strong clustering process in Po, Rn, and Ra isotopes. Our calculations predict a similar feature for superheavy nuclei.

Therefore in our calculations we used the parameters $f_m=0.83$, $\chi_m=55$. For the proportionality coefficient in Eq. (3.7) the regression analysis gives the value $f_1=8.0\ 10^{-4}$. In Figs. 10(a) and 10(b) we plotted the dependence of the parameters γ_0,γ_1 upon the neutron number along the even-even α-chains in Table II. The improvement, especially for the slope γ_1, is obvious. Now the ratio to the experimental width is described within a factor of 3 for most of decays.

A similar improvement (except the vicinity of semimagic neutron numbers) is shown in Figs. 11(a) and 11(b) for even-odd favored α chains in Table II. Here we used a larger value $f_m=0.84$, corresponding to the maximum $\gamma_0(\max)=0$, but the same values of f_1,χ_m.

From the analysis of Figs. 10 and 11 one remarks that in the superheavy region we still underestimated the slope parameter for both cases. The situation here can be improved by assuming a quadratic dependence of the coefficient f_1 upon the number of clusters $N_\alpha=(N-N_0)/2$ with $N_0=126$, namely,

$$f_1 \rightarrow f_1 + f_2 N_\alpha^2. \tag{3.10}$$

We remind here that a quadratic in N_α dependence of the Q value was empirically found in Ref. [1]. We stress on the fact that this kind of dependence affects only the superheavy region, with large values of N_α. The results are given in Figs. 12(a) and 12(b) for even-even chains and in Figs. 13(a) and 13(b) for even-odd chains. We considered a correcting term with $f_2=1.28\ 10^{-6}$. The improvement of the slope parameter in the superheavy region is obvious. The mean value of this parameter and its standard deviation for even-even chains is $\gamma_1=-0.001\pm0.034$, while for even-odd chains we obtained $\gamma_1=-0.012\pm0.033$.

The quadratic dependence in Eq. (3.10) can be also interpreted in terms of the total number of interacting clustering

TABLE III. Parameters of the preformation amplitude according to Eqs. (3.7) and (3.10).

Interval	Nucleus	f_m	f_1	f_2	χ_m	P_{min}
$N<126$	Even-even	0.80	8.0×10^{-4}	0	40	0.025
	Even-odd	0.80	8.0×10^{-4}	0	40	0.025
$N>126$	Even-even	0.83	8.0×10^{-4}	1.28×10^{-6}	55	0.025
	Even-odd	0.84	8.0×10^{-4}	1.28×10^{-6}	55	0.025

TABLE IV. Even-even α-decay chains in heavy and superheavy nuclei. The quadrupole deformations β_2 and FRLDM Q-values E are taken from Ref. [47].

Z	N	A	I	β_2	E (MeV)	χ	f	γ_1	$\log_{10}T$ (s)	$\log_{10}T_{\rm exp}$ (s)	S_α
92	130	222	38	0.048	9.436	36.587	0.815	0.043	−5.076	−6.000	0.0086
90	130	220	40	0.030	8.988	36.652	0.815	−0.016	−4.459	−5.013	0.0085
92	132	224	40	0.146	8.660	38.195	0.816	0.059	−3.217	−3.155	0.0073
102	142	244	40	0.224	9.606	40.325	0.817	0.078	−2.759		0.0070
104	144	248	40	0.225	10.246	39.831	0.816	0.043	−3.702		0.0074
106	146	252	40	0.236	10.406	40.304	0.816	0.102	−3.575		0.0072
108	148	256	40	0.237	10.966	40.022	0.816	0.135	−4.310		0.0075
110	150	260	40	0.228	11.846	39.238	0.814	0.119	−5.554		0.0084
112	152	264	40	0.228	12.826	38.412	0.813	0.145	−6.929		0.0101
88	130	218	42	0.020	8.581	36.655	0.815	0.018	−4.124	−4.585	0.0086
90	132	222	42	0.111	8.164	38.460	0.817	−0.003	−2.358	−2.553	0.0070
92	134	226	42	0.172	7.600	40.775	0.818	0.022	0.005	−0.301	0.0062
102	144	246	42	0.224	9.476	40.603	0.817	0.056	−2.407		0.0071
104	146	250	42	0.235	9.746	40.843	0.817	0.069	−2.521		0.0070
106	148	254	42	0.237	10.116	40.880	0.817	0.095	−2.865		0.0071
108	150	258	42	0.238	10.586	40.736	0.816	0.101	−3.446		0.0075
110	152	262	42	0.228	11.896	39.158	0.814	0.104	−5.688		0.0091
112	154	266	42	0.219	12.976	38.191	0.812	0.095	−7.196		0.0112
114	156	270	42	0.200	13.416	38.247	0.812	0.106	−7.489		0.0145
86	130	216	44	0.008	8.235	36.544	0.815	−0.035	−3.673	−4.347	0.0092
88	132	220	44	0.103	7.627	38.884	0.817	−0.018	−1.331	−1.638	0.0068
90	134	224	44	0.164	7.355	40.524	0.818	−0.026	0.229	0.114	0.0062
92	136	228	44	0.191	6.836	42.996	0.820	−0.014	2.922	2.903	0.0055
94	138	232	44	0.208	6.753	44.228	0.821	0.005	3.995	4.000	0.0052
98	142	240	44	0.215	7.758	43.070	0.819	0.007	1.539	1.806	0.0058
102	146	248	44	0.235	8.966	41.745	0.818	0.017	−1.033		0.0067
104	148	252	44	0.236	9.546	41.271	0.817	0.028	−2.020		0.0070
106	150	256	44	0.247	9.526	42.130	0.817	0.049	−1.351		0.0066
108	152	260	44	0.239	10.646	40.624	0.815	0.033	−3.579		0.0080
110	154	264	44	0.229	12.096	38.835	0.813	0.005	−6.047		0.0104
112	156	268	44	0.220	12.686	38.628	0.812	−0.001	−6.629		0.0117
114	158	272	44	0.201	12.926	38.967	0.812	0.087	−6.699		0.0149
116	160	276	44	0.192	13.286	39.126	0.811	0.121	−6.986		0.0225
86	132	218	46	0.040	7.299	38.820	0.817	0.014	−0.917	−1.456	0.0072
88	134	222	46	0.130	6.710	41.459	0.819	0.012	1.923	1.591	0.0057
90	136	226	46	0.173	6.487	43.153	0.820	−0.045	3.706	3.398	0.0053
92	138	230	46	0.199	6.029	45.787	0.822	−0.041	6.617	6.431	0.0047
94	140	234	46	0.216	6.345	45.631	0.822	−0.010	5.852	5.903	0.0047
96	142	238	46	0.215	6.670	45.480	0.822	0.000	5.155	4.954	0.0047
98	144	242	46	0.224	7.549	43.666	0.820	−0.017	2.342	2.477	0.0056
100	146	246	46	0.234	8.417	42.220	0.818	−0.016	0.070	0.079	0.0065
102	148	250	46	0.235	8.383	43.175	0.819	−0.067	0.891		0.0061
104	150	254	46	0.237	9.036	42.423	0.818	−0.037	−0.501		0.0067
106	152	258	46	0.248	9.456	42.288	0.817	−0.039	−1.049		0.0069
108	154	262	46	0.239	10.866	40.213	0.814	−0.082	−3.924		0.0089
110	156	266	46	0.220	11.786	39.344	0.813	−0.089	−5.265		0.0107

TABLE IV. (*Continued.*)

Z	N	A	I	β_2	E (MeV)	χ	f	γ_1	$\log_{10}T$ (s)	$\log_{10}T_{\mathrm{exp}}$ (s)	S_α
112	158	270	46	0.220	12.096	39.561	0.813	−0.038	−5.476		0.0118
114	160	274	46	0.201	12.486	39.650	0.812	0.026	−5.906		0.0157
116	162	278	46	0.193	13.036	39.502	0.811	0.007	−6.521		0.0260
118	164	282	46	0.062	12.916	40.385	0.812	0.144	−5.811		0.0397
86	134	220	48	0.111	6.438	41.338	0.819	0.011	2.237	1.748	0.0060
88	136	224	48	0.164	5.823	44.509	0.821	0.035	5.824	5.519	0.0049
90	138	228	48	0.182	5.555	46.637	0.823	0.045	8.147	7.919	0.0044
92	140	232	48	0.207	5.450	48.161	0.824	0.000	9.765	9.505	0.0040
94	142	236	48	0.215	5.904	47.308	0.823	−0.022	8.131	8.114	0.0041
96	144	240	48	0.224	6.436	46.302	0.822	−0.045	6.318	6.519	0.0044
98	146	244	48	0.234	7.370	44.196	0.820	−0.021	3.078	3.204	0.0054
100	148	248	48	0.235	8.040	43.202	0.819	−0.041	1.298	1.653	0.0061
102	150	252	48	0.236	8.593	42.647	0.818	−0.048	0.197	0.602	0.0067
104	152	256	48	0.247	8.995	42.522	0.817	−0.031	−0.434	−0.444	0.0071
106	154	260	48	0.239	9.967	41.192	0.815	−0.064	−2.424	−2.060	0.0083
108	156	264	48	0.229	11.042	39.893	0.814	−0.093	−4.331	−4.000	0.0102
110	158	268	48	0.221	10.062	42.584	0.816	−0.029	−1.379		0.0081
112	160	272	48	0.221	11.606	40.389	0.813	−0.099	−4.463		0.0123
114	162	276	48	0.212	12.336	39.893	0.812	−0.103	−5.506		0.0186
116	164	280	48	0.062	12.426	40.462	0.812	−0.006	−5.259		0.0307
118	166	284	48	0.062	13.096	40.109	0.810	−0.011	−6.141		0.0585
86	136	222	50	0.137	5.623	44.236	0.821	0.071	5.913	5.519	0.0051
88	138	226	50	0.172	4.904	48.504	0.825	0.053	11.190	10.724	0.0039
90	140	230	50	0.198	4.806	50.143	0.826	0.044	12.879	12.491	0.0036
92	142	234	50	0.215	4.895	50.822	0.826	0.016	13.317	13.041	0.0034
94	144	238	50	0.215	5.631	48.445	0.824	0.001	9.598	9.591	0.0037
96	146	242	50	0.224	6.254	46.974	0.823	−0.018	7.151	7.279	0.0041
98	148	246	50	0.234	6.901	45.676	0.821	−0.018	4.947	5.204	0.0048
100	150	250	50	0.235	7.592	44.461	0.820	−0.027	2.959	3.301	0.0056
102	152	254	50	0.246	8.264	43.490	0.818	−0.027	1.317	1.857	0.0065
104	154	258	50	0.238	8.656	43.349	0.818	−0.120	0.800		0.0069
106	156	262	50	0.229	9.606	41.962	0.816	−0.060	−1.380		0.0084
108	158	266	50	0.230	9.686	42.597	0.816	−0.029	−0.972		0.0082
110	160	270	50	0.221	10.316	42.059	0.815	0.004	−1.918		0.0097
112	162	274	50	0.222	11.396	40.762	0.813	−0.083	−3.996		0.0138
114	164	278	50	0.193	12.646	39.403	0.810	−0.131	−6.117		0.0260
116	166	282	50	0.062	11.646	41.797	0.813	−0.098	−3.564		0.0357
118	168	286	50	0.080	13.046	40.188	0.810	−0.114	−6.027		0.0762
90	142	232	52	0.207	4.115	54.194	0.829	0.062	18.243	17.756	0.0029
92	144	236	52	0.215	4.608	52.385	0.828	0.064	15.295	15.000	0.0030
94	146	240	52	0.223	5.293	49.971	0.825	0.015	11.610	11.447	0.0033
96	148	244	52	0.234	5.940	48.203	0.824	0.000	8.720	8.875	0.0037
98	150	248	52	0.235	6.404	47.418	0.823	−0.007	7.226	7.544	0.0042
100	152	252	52	0.245	7.194	45.677	0.821	−0.030	4.501	5.041	0.0052
102	154	256	52	0.237	8.606	42.620	0.817	−0.021	0.176	0.613	0.0076
104	156	260	52	0.228	8.569	43.571	0.818	−0.020	0.970		0.0073
106	158	264	52	0.229	8.706	44.080	0.818	−0.015	1.187		0.0074

TABLE IV. (*Continued.*)

Z	N	A	I	β_2	E (MeV)	χ	f	γ_1	$\log_{10}T$ (s)	$\log_{10}T_{\mathrm{exp}}$ (s)	S_α
108	160	268	52	0.230	8.996	44.203	0.817	−0.017	0.957		0.0080
110	162	272	52	0.222	10.026	42.665	0.815	−0.024	−1.346		0.0111
112	164	276	52	0.212	11.846	39.982	0.811	−0.078	−5.016		0.0207
114	166	280	52	0.053	11.606	41.133	0.812	−0.081	−3.903		0.0284
116	168	284	52	0.071	11.606	41.871	0.812	−0.095	−3.590		0.0465
118	170	288	52	0.080	12.876	40.454	0.809	−0.137	−5.779		0.0909
92	146	238	54	0.215	4.304	54.207	0.829	0.041	17.762	17.255	0.0025
94	148	242	54	0.224	5.020	51.315	0.826	−0.003	13.430	13.176	0.0028
96	150	246	54	0.234	5.513	50.039	0.825	−0.006	11.171	11.279	0.0032
98	152	250	54	0.245	6.169	48.316	0.823	−0.022	8.381	8.690	0.0040
100	154	254	54	0.237	7.345	45.208	0.820	−0.015	3.856	4.146	0.0059
102	156	258	54	0.228	8.120	43.879	0.818	0.033	1.752		0.0073
104	158	262	54	0.229	7.916	45.336	0.819	0.005	3.141		0.0066
106	160	266	54	0.230	8.026	45.912	0.819	−0.001	3.456		0.0068
108	162	270	54	0.231	8.696	44.961	0.818	−0.024	1.842		0.0087
110	164	274	54	0.222	10.506	41.682	0.813	−0.067	−2.674		0.0165
112	166	278	54	0.164	12.296	39.246	0.809	−0.150	−5.909		0.0315
114	168	282	54	0.053	10.006	44.302	0.815	−0.100	0.003		0.0243
116	170	286	54	0.080	11.416	42.220	0.812	−0.102	−3.197		0.0539
118	172	290	54	−0.112	12.806	40.567	0.809	−0.085	−5.797		0.1056
94	150	244	56	0.224	4.703	53.020	0.828	0.049	15.598	15.505	0.0024
96	152	248	56	0.235	5.200	51.526	0.826	0.028	13.163	13.146	0.0028
98	154	252	56	0.236	6.257	47.978	0.823	0.009	7.904	8.000	0.0043
100	156	256	56	0.227	7.065	46.098	0.820	0.019	4.993	5.079	0.0058
102	158	260	56	0.228	7.412	45.930	0.820	0.034	4.303		0.0064
104	160	264	56	0.220	7.326	47.129	0.821	0.010	5.447		0.0061
106	162	268	56	0.231	7.596	47.196	0.821	0.001	5.080		0.0069
108	164	272	56	0.222	9.206	43.700	0.816	−0.034	0.183		0.0130
110	166	276	56	0.212	10.726	41.254	0.812	−0.033	−3.255		0.0238
112	168	280	56	0.080	11.126	41.260	0.811	−0.017	−3.450		0.0316
114	170	284	56	0.062	9.436	45.622	0.817	−0.056	1.588		0.0242
116	172	288	56	−0.104	11.316	42.409	0.811	−0.086	−3.084		0.0604
118	174	292	56	0.081	12.366	41.284	0.809	−0.078	−4.925		0.1056
96	154	250	58	0.225	5.208	51.490	0.826	0.045	13.105	12.477	0.0029
98	156	254	58	0.226	5.967	49.134	0.824	0.052	9.437	9.301	0.0041
100	158	258	58	0.228	6.749	47.168	0.821	0.032	6.237		0.0056
102	160	262	58	0.219	6.586	48.728	0.823	0.051	7.968		0.0052
104	162	266	58	0.230	6.736	49.152	0.823	−0.045	8.124		0.0056
106	164	270	58	0.221	8.156	45.550	0.818	0.018	2.897		0.0106
108	166	274	58	0.212	9.466	43.098	0.814	−0.015	−0.666		0.0189
110	168	278	58	0.155	10.406	41.886	0.812	−0.041	−2.505		0.0284
112	170	282	58	0.089	9.416	44.853	0.816	−0.014	0.987		0.0230
114	172	286	58	−0.096	9.386	45.746	0.816	−0.041	1.638		0.0269
116	174	290	58	0.072	11.116	42.791	0.811	−0.039	−2.672		0.0640
102	162	264	60	0.220	6.006	51.030	0.825	−0.012	10.920		0.0046
104	164	268	60	0.221	7.156	47.691	0.821	0.019	6.018		0.0083
106	166	272	60	0.201	8.386	44.923	0.817	0.001	1.991		0.0151

TABLE IV. (*Continued.*)

Z	N	A	I	β_2	E (MeV)	χ	f	γ_1	$\log_{10}T$ (s)	$\log_{10}T_{\rm exp}$ (s)	S_α
108	168	276	60	0.164	9.316	43.446	0.814	−0.025	−0.256		0.0230
110	170	280	60	0.108	9.046	44.927	0.816	−0.019	1.384		0.0221
112	172	284	60	0.081	9.130	45.555	0.816	−0.026	1.859	1.255	0.0236
114	174	288	60	0.053	9.800	44.774	0.814	−0.032	0.340	0.661	0.0346
116	176	292	60	−0.070	10.540	43.949	0.812	−0.017	−1.293	−1.260	0.0596

pairs, namely, $N_\alpha^2 \approx 2N_\alpha(N_\alpha-1)/2$. Thus, our analysis based on the logarithmic derivative continuity, shows very clearly that the effect of the α-clusterizations becomes much stronger for superheavy nuclei. Their half-lives are practically not influenced, but their radial tails should be significantly larger than those predicted by standard shell-model calculations.

We stress on the fact that this correction procedure has a relative character, depending upon the values f_m, χ_m. We remind that f_1, f_2, f_m are the only free parameters of this model and χ_m is dependent upon f_m. They are directly connected with the radial shape of the α-particle preformation amplitude. Any other parameters are taken from independent calculations. We also remind that a similar technique, i.e., the use of a variable cluster ho parameter, was used in Ref. [42].

E. Systematics in the region $82<Z<118$

We summarize in Table III the parameters we used to correct the shell-model estimate of the α-preformation amplitude. We used these values to compute the measured half-lives of even-even and even-odd α emitters in the region $Z>82$. At the same time we predicted the half-life and the slope parameter for all possible superheavy nuclei with $Z>102$. The results are given in Table IV for even-even nuclei and Table V for even-odd nuclei. Here we give the computed logarithm of the half-life and also its slope with respect to the matching radius R, according to Eq. (3.3). The Q values were estimated using experimental binding energies or FRLDM estimates of Ref. [47]. The quadrupole deformation parameters are taken from the same reference.

A very important accuracy test of our calculations is the value of the slope parameter γ_1, which should vanish. As we showed in the preceding section this gives the measure of selfconsistency between the internal preformation factor and the used α-decay Q value. One can see that for most of the predicted values the slope parameter is rather small. In other words we can obtain Q values in Tables IV and V within the precision of 500 keV, i.e., $|\gamma_1| \leqslant 0.02$, for many of the analyzed decays by solving Eq. (3.4). For the remaining cases our parametrization is not consistent with the Q values taken from Ref. [47]. The conclusion is that these values should be more carefully analyzed.

In the last column we give the spectroscopic factors defined as the integral over the preformation factor squared. The values are in agreement with those predicted in Ref. [53], i.e., $S_\alpha \approx 10^{-2}$, for $Z \leqslant 110$ and increase for heavier nuclei. This feature is obviously connected with their larger radial tails.

IV. CONCLUSIONS

We analyzed in this paper the α clustering, using the decay widths for deformed even-even and favored even-odd emitters with $Z>82$. The α-particle preformation amplitude was estimated within the pairing approach. We used the universal parametrization of the mean field and the empirical rule for the gap parameter $\Delta = 12/\sqrt{A}$. Due to a coherent superposition of many spherical configuration the preformation factor is not sensitive to the local fluctuation of these parameters.

The penetration part was computed within the deformed WKB approach. We showed that the decay width increases by a factor between three and five for the largest deformation $\beta_2 = 0.3$, depending on the mass number.

It turns out that the decay width is very sensitive to the sp ho parameter and the number of considered spherical configurations. They simultaneously determine the order of magnitude and the slope of the decay width with respect to the matching radius, giving the plateau condition. It is possible to describe all α-decay widths within a factor of 2 for $Z>82$, $82<N<126$, by using a constant, but smaller ho parameter $\beta = 0.80\beta_N$ and $P_{\rm min} = 0.025$. This behavior is related with the almost constant value of the Coulomb parameter in this region.

It turns out that the slope of the decay width versus the matching radius has a strong variation for $N>126$, in an obvious correlation with the Coulomb parameter. Thus, the relative amount of the α clustering here cannot be described only within the pairing approach and an additional mechanism is necessary. In order to restore the plateau condition we proposed a simple procedure. We supposed a cluster factor, multiplying the preformation amplitude. It contains exponentially an ho parameter, proportional to the Coulomb parameter. This ansatz is suggested by a similar exponential dependence of the Coulomb function upon this parameter. Therefore the energy of the emitted particle contains two terms, namely, a smooth part and a cluster correction. This procedure, applied for the interval $82<N<126$, reproduces practically the previous results.

The method improves simultaneously the ratio to the experimental width and the slope with respect to the matching radius. The relative increase of the α clustering is related to the decrease of the Coulomb parameter. It is stronger for two regions, namely, above $N=126$ and in superheavy nuclei. It has a minimum around $N=152$.

An additional dependence upon the number of interacting α particles improves the plateau condition for superheavy nuclei. This additional clustering, which seems to be very

TABLE V. Even-odd α-decay chains in heavy and superheavy nuclei.

Z	N	A	I	β_2	E (MeV)	χ	f	γ_1	$\log_{10}T$ (s)	$\log_{10}T_{\mathrm{exp}}$ (s)	S_α
92	131	223	39	0.110	8.977	37.513	0.826	0.022	−3.736	−4.699	0.0074
90	131	221	41	0.102	7.911	39.069	0.827	0.018	−1.300	−1.553	0.0067
92	133	225	41	0.165	8.054	39.607	0.827	−0.009	−1.163	−1.301	0.0065
94	135	229	41	0.190	7.592	41.708	0.829	−0.008	0.994		0.0059
96	137	233	41	0.207	7.439	43.057	0.830	0.045	2.177		0.0056
98	139	237	41	0.215	8.166	41.976	0.829	0.065	0.317		0.0062
100	141	241	41	0.224	8.616	41.723	0.828	0.037	−0.364		0.0063
102	143	245	41	0.224	9.446	40.666	0.827	0.059	−2.103		0.0067
104	145	249	41	0.225	10.126	40.068	0.826	−0.011	−3.148		0.0071
106	147	253	41	0.236	10.156	40.798	0.827	0.089	−2.743		0.0068
108	149	257	41	0.238	10.856	40.225	0.826	0.081	−3.823		0.0073
110	151	261	41	0.228	11.746	39.406	0.824	0.085	−5.101		0.0083
112	153	265	41	0.219	12.956	38.220	0.823	0.085	−6.844		0.0103
114	155	269	41	0.210	13.596	37.992	0.822	0.114	−7.537		0.0138
88	131	219	43	0.077	7.857	38.309	0.827	−0.023	−1.707	−1.824	0.0070
90	133	223	43	0.138	7.455	40.249	0.828	−0.034	0.194	0.041	0.0061
92	135	227	43	0.182	7.029	42.400	0.830	−0.021	2.389	1.820	0.0055
98	141	239	43	0.215	7.799	42.955	0.829	0.000	1.654	1.623	0.0058
100	143	243	43	0.224	8.730	41.452	0.828	−0.004	−0.719	−0.347	0.0066
102	145	247	43	0.224	9.356	40.864	0.827	0.011	−1.820		0.0068
104	147	251	43	0.236	9.526	41.313	0.827	0.005	−1.537		0.0067
106	149	255	43	0.247	9.886	41.354	0.827	0.040	−2.001		0.0068
108	151	259	43	0.238	10.506	40.892	0.826	0.013	−2.938		0.0073
110	153	263	43	0.228	12.096	38.834	0.823	0.006	−5.712		0.0095
112	155	267	43	0.219	12.766	38.505	0.822	−0.026	−6.414		0.0109
114	157	271	43	0.200	13.196	38.566	0.822	0.065	−6.803		0.0141
116	159	275	43	0.192	13.446	38.892	0.822	0.105	−6.925		0.0208
86	131	217	45	0.039	7.920	37.266	0.826	−0.036	−2.513	−3.268	0.0080
88	133	221	45	0.111	6.764	41.292	0.829	−0.011	2.087	1.903	0.0057
90	135	225	45	0.165	6.631	42.680	0.830	−0.016	3.282	3.000	0.0053
92	137	229	45	0.191	6.509	44.065	0.831	−0.056	4.539	4.431	0.0051
94	139	233	45	0.207	6.447	45.267	0.832	−0.042	5.609	6.000	0.0048
98	143	241	45	0.224	7.498	43.812	0.830	−0.027	2.813	3.301	0.0054
100	145	245	45	0.234	8.326	42.449	0.829	−0.043	0.675	0.623	0.0062
102	147	249	45	0.235	9.016	41.630	0.827	−0.028	−0.742		0.0067
104	149	253	45	0.236	9.326	41.756	0.827	−0.035	−0.978		0.0066
106	151	257	45	0.247	9.406	42.399	0.827	−0.019	−0.618		0.0064
108	153	261	45	0.239	10.836	40.267	0.825	−0.102	−3.535		0.0083
110	155	265	45	0.229	11.886	39.177	0.823	−0.106	−5.199		0.0100
112	157	269	45	0.220	12.426	39.031	0.822	−0.023	−5.866		0.0113
114	159	273	45	0.201	12.696	39.320	0.822	0.000	−5.969		0.0146
116	161	277	45	0.192	13.166	39.305	0.821	0.040	−6.459		0.0230
118	163	281	45	0.184	13.796	39.075	0.820	0.120	−7.125		0.0383
86	133	219	47	0.103	6.577	40.897	0.828	0.022	1.910	1.724	0.0060
90	137	227	47	0.173	5.895	45.270	0.832	−0.042	6.751	6.903	0.0047
94	141	235	47	0.215	5.989	46.969	0.833	−0.057	7.894	7.748	0.0042
98	145	243	47	0.234	7.218	44.657	0.831	−0.019	3.863	3.806	0.0051

TABLE V. (*Continued.*)

Z	N	A	I	β_2	E (MeV)	χ	f	γ_1	$\log_{10}T$ (s)	$\log_{10}T_{\mathrm{exp}}$ (s)	S_α
100	147	247	47	0.234	8.040	43.200	0.829	−0.030	1.602	2.000	0.0059
102	149	251	47	0.236	8.781	42.186	0.828	−0.079	−0.073		0.0067
104	151	255	47	0.246	8.897	42.754	0.828	−0.028	0.196	0.653	0.0063
106	153	259	47	0.248	9.126	43.047	0.828	−0.023	0.215	0.699	0.0064
108	155	263	47	0.239	10.706	40.513	0.825	−0.131	−3.224		0.0087
110	157	267	47	0.220	11.600	39.662	0.823	−0.078	−4.784	−5.523	0.0104
112	159	271	47	0.221	11.836	39.994	0.823	−0.080	−4.630		0.0115
114	161	275	47	0.212	12.456	39.699	0.822	−0.065	−5.476		0.0162
116	163	279	47	0.193	12.996	39.564	0.821	0.000	−6.133		0.0280
118	165	283	47	0.062	12.706	40.719	0.822	−0.013	−5.110		0.0433
90	139	229	49	0.190	4.966	49.327	0.835	0.003	12.020	11.613	0.0038
92	141	233	49	0.207	4.945	50.563	0.836	0.007	13.157	12.778	0.0035
94	143	237	49	0.215	5.281	50.022	0.836	−0.009	11.894	12.000	0.0034
96	145	241	49	0.223	6.078	47.648	0.833	−0.015	8.328	8.613	0.0038
98	147	245	49	0.234	7.295	44.424	0.830	−0.020	3.589	3.954	0.0052
100	149	249	49	0.235	7.694	44.164	0.829	−0.009	2.827	3.000	0.0055
102	151	253	49	0.236	8.022	44.143	0.829	−0.031	2.389	1.630	0.0057
104	153	257	49	0.238	8.794	43.006	0.828	−0.028	0.431	1.623	0.0067
106	155	261	49	0.238	9.753	41.643	0.826	−0.029	−1.654	−0.398	0.0079
108	157	265	49	0.230	10.564	40.787	0.824	−0.076	−2.935	−2.699	0.0092
110	159	269	49	0.221	11.110	40.530	0.823	−0.064	−3.624	−3.770	0.0103
112	161	273	49	0.221	11.506	40.566	0.823	−0.077	−3.998		0.0125
114	163	277	49	0.202	12.326	39.910	0.821	−0.119	−5.185		0.0202
116	165	281	49	0.062	12.166	40.893	0.822	−0.065	−4.268		0.0330
118	167	285	49	0.071	13.066	40.156	0.820	−0.030	−5.823		0.0647
92	143	235	51	0.215	4.325	54.070	0.839	0.016	17.833	17.591	0.0028
94	145	239	51	0.223	5.281	50.026	0.835	0.003	11.943	12.000	0.0033
96	147	243	51	0.234	5.921	48.279	0.834	0.008	8.981	9.079	0.0036
98	149	247	51	0.234	6.444	47.269	0.833	0.008	7.156	7.505	0.0041
100	151	251	51	0.245	6.984	46.357	0.831	0.010	5.474	6.079	0.0047
102	153	255	51	0.237	7.937	44.378	0.829	−0.009	2.681	3.531	0.0060
104	155	259	51	0.239	8.951	42.630	0.827	−0.006	0.101	0.778	0.0075
106	157	263	51	0.229	9.244	42.777	0.826	0.009	−0.121	0.477	0.0079
108	159	267	51	0.230	9.346	43.366	0.827	−0.013	0.220		0.0077
110	161	271	51	0.221	10.710	41.282	0.824	−0.029	−2.731		0.0111
112	163	275	51	0.222	11.496	40.585	0.822	−0.056	−3.979		0.0154
114	165	279	51	−0.052	12.036	40.390	0.821	−0.060	−4.496		0.0261
116	167	283	51	0.062	11.806	41.514	0.822	−0.027	−3.621		0.0412
118	169	287	51	−0.104	12.876	40.453	0.820	−0.200	−5.356		0.0785
94	147	241	53	0.224	5.017	51.329	0.837	0.027	13.592	13.362	0.0029
96	149	245	53	0.234	5.489	50.146	0.835	0.018	11.429	11.462	0.0031
98	151	249	53	0.235	5.946	49.212	0.834	0.022	9.709	10.114	0.0035
100	153	253	53	0.236	6.824	46.901	0.832	−0.016	6.369	6.968	0.0047
102	155	257	53	0.238	8.392	43.161	0.827	−0.003	0.924	1.699	0.0073
104	157	261	53	0.228	8.452	43.873	0.828	0.036	1.504	1.903	0.0072
106	159	265	53	0.229	8.770	43.923	0.827	0.024	1.263	1.382	0.0078
108	161	269	53	0.231	9.170	43.785	0.827	0.025	0.681	0.851	0.0088

TABLE V. (*Continued.*)

Z	N	A	I	β_2	E (MeV)	χ	f	γ_1	$\log_{10}T$ (s)	$\log_{10}T_{\mathrm{exp}}$ (s)	S_α
110	163	273	53	0.222	9.730	43.313	0.826	−0.043	−0.276	−0.921	0.0113
112	165	277	53	0.202	11.650	40.321	0.821	−0.073	−4.454	−3.319	0.0222
114	167	281	53	0.053	10.936	42.375	0.823	−0.045	−2.114		0.0270
116	169	285	53	0.071	11.456	42.146	0.822	−0.120	−2.923		0.0480
118	171	289	53	0.080	12.756	40.645	0.819	−0.053	−5.249		0.0911
96	151	247	55	0.235	4.988	52.608	0.838	−0.004	14.744	14.839	0.0025
98	153	251	55	0.236	5.809	49.793	0.835	−0.009	10.628	10.908	0.0035
100	155	255	55	0.237	7.175	45.742	0.830	0.020	4.633	4.886	0.0056
102	157	259	55	0.228	7.659	45.182	0.829	0.049	3.503	4.079	0.0064
104	159	263	55	0.229	7.596	46.282	0.830	0.056	4.609		0.0062
106	161	267	55	0.230	7.856	46.407	0.830	0.037	4.351		0.0067
108	163	271	55	0.222	8.826	44.630	0.827	0.001	1.706		0.0098
110	165	275	55	0.221	10.736	41.234	0.822	−0.009	−3.015		0.0196
112	167	279	55	0.164	11.816	40.036	0.820	−0.030	−4.820		0.0316
114	169	283	55	0.053	9.576	45.286	0.826	−0.030	1.502		0.0227
116	171	287	55	0.080	11.296	42.445	0.822	−0.087	−2.642		0.0538
118	173	291	55	0.081	12.556	40.969	0.819	−0.020	−5.021		0.1014
98	155	253	57	0.226	6.115	48.534	0.833	0.034	8.768	8.716	0.0042
100	157	257	57	0.227	6.663	47.470	0.832	0.043	6.871	6.968	0.0051
102	159	261	57	0.219	7.159	46.736	0.831	0.049	5.526		0.0060
104	161	265	57	0.220	6.996	48.229	0.832	0.044	7.110		0.0056
106	163	269	57	0.222	8.740	44.000	0.826	0.035	1.248		0.0110
108	165	273	57	0.221	9.780	42.400	0.824	−0.005	−1.284		0.0173
110	167	277	57	0.173	10.180	42.347	0.823	−0.017	−1.731		0.0226
112	169	281	57	0.089	10.670	42.136	0.822	−0.016	−2.297		0.0298
114	171	285	57	−0.096	11.310	41.675	0.821	−0.034	−3.323		0.0441
116	173	289	57	0.080	11.630	41.835	0.820	−0.007	−3.615		0.0670
118	175	293	57	0.080	12.370	41.280	0.818	0.014	−4.731		0.1067
102	161	263	59	0.220	6.336	49.682	0.834	0.041	9.359		0.0049
104	163	267	59	0.221	6.836	48.793	0.832	0.017	7.755		0.0064
106	165	271	59	0.212	8.406	44.869	0.827	0.028	2.178		0.0129
108	167	275	59	0.183	9.396	43.260	0.824	0.004	−0.242		0.0203
110	169	279	59	0.127	9.676	43.438	0.824	0.008	−0.308		0.0242
112	171	283	59	0.089	9.016	45.838	0.827	−0.003	2.446		0.0207
114	173	287	59	−0.078	10.290	43.694	0.823	−0.007	−0.756	0.740	0.0372
116	175	291	59	0.072	11.116	42.792	0.821	0.020	−2.429		0.0648
118	177	295	59	−0.087	12.186	41.591	0.818	0.023	−4.409		0.1163
102	163	265	61	0.221	6.046	50.862	0.835	−0.044	10.919		0.0051
104	165	269	61	0.212	7.376	46.975	0.830	0.038	5.262		0.0101
106	167	273	61	0.183	8.266	45.249	0.827	0.022	2.636		0.0159
108	169	277	61	0.145	8.746	44.841	0.826	0.003	1.788		0.0201
110	171	281	61	0.108	8.830	45.476	0.826	−0.001	2.331	1.982	0.0211
112	173	285	61	0.089	8.670	46.749	0.828	−0.083	3.720	2.966	0.0202
114	175	289	61	−0.052	9.710	44.982	0.824	0.021	0.851	1.483	0.0346
116	177	293	61	−0.070	10.936	43.144	0.821	0.033	−2.062		0.0698
118	179	297	61	−0.035	12.646	40.829	0.816	0.030	−5.413		0.1565

strong, may affect the stability of nuclei in this region.

Based on this parametrization we gave predictions for half-lives, concerning even-even and even-odd superheavy α emitters with $Z>102$. The predicted values for the slope parameter are in general small for many nuclei. They show the consistency between the corrected α-particle microscopic preformation factor and the Q value.

Our future task is to perform a complete microscopic analysis of the cluster component in terms of two-proton and two-neutron collective states, including magic nuclei, in analogy with the approach of Ref. [33]. Thus, the analysis of decay processes along α chains seems to be a nontrivial tool to investigate the amount of clustering in heavy and superheavy nuclei.

ACKNOWLEDGMENT

We acknowledge fruitful discussions with J. Hopiavuori (Jyväskylaä).

[1] G. Dussel, E. Caurier, and A. P. Zuker, At. Data Nucl. Data Tables **39**, 205 (1988).
[2] Y. K. Gambhir, P. Ring, and P. Schuck, Phys. Rev. Lett. **51**, 1235 (1983).
[3] G. Gamow, Z. Phys. **51**, 204 (1928).
[4] D. F. Jackson and M. Rhoades-Brown, Ann. Phys. (N.Y.) **105**, 151 (1977).
[5] D. F. Jackson and M. Rhoades-Brown, J. Phys. G **4**, 1441 (1978).
[6] T. Berggren and P. Olanders, Nucl. Phys. **473**, 189 (1987).
[7] B. Buck, A. C. Merchand, and S. M. Perez, At. Data Nucl. Data Tables **54**, 52 (1993).
[8] G. Breit, *Theory of Resonant Reactions and Allied Topics* (Springer-Verlag, Berlin, 1959).
[9] P. O. Fröman, Mat. Fys. Medd. K. Dan. Vidensk. Selsk. **1**, 1 (1957).
[10] G. N. Flerov, At. Energ. **26**, 138 (1969).
[11] A. Sandulescu, R. K. Gupta, W. Scheid, and W. Greiner, Phys. Lett. **60B**, 225 (1976).
[12] R. K. Gupta, A. Sandulescu, and W. Greiner, Phys. Lett. **67B**, 257 (1977).
[13] R. Smolanczuk, Phys. Rev. C **56**, 812 (1997).
[14] A. Sobiczewski, I. Muntian, and Z. Patyk, Phys. Rev. C **63**, 034306 (2001).
[15] G. Royer, J. Phys. G **26**, 1149 (2000).
[16] G. Royer and R. Gherghescu, Nucl. Phys. **A699**, 479 (2002).
[17] S. Kumar, M. Balasubramaniam, R. K. Gupta, G. Münzenberg, and W. Scheid, J. Phys. G **29**, 625 (2003).
[18] S. Typel and B. A. Brown, Phys. Rev. C **67**, 034313 (2003).
[19] I. Silisteanu and W. Scheid, Nucl. Phys. A (to be submitted).
[20] R. G. Thomas, Prog. Theor. Phys. **12**, 253 (1954).
[21] A. M. Lane and R. G. Thomas, Rev. Mod. Phys. **30**, 257 (1958).
[22] A. Sandulescu, Nucl. Phys. **A37**, 332 (1962).
[23] H. J. Mang, Phys. Rev. **119**, 1069 (1960).
[24] H. J. Mang, Annu. Rev. Nucl. Sci. **14**, 1 (1964); H. J. Mang and J. O. Rasmussen, Mat. Fys. Medd. K. Dan. Vidensk. Selsk. **2**, 1 (1962); J. K. Poggenburg, H. J. Mang, and J. O. Rasmussen, Phys. Rev. **181**, 1697 (1969).
[25] R. G. Lovas, R. J. Liotta, A. Insolia, K. Varga, and D. S. Delion, Phys. Rep. **294**, 265 (1998).
[26] V. G. Soloviev, Phys. Lett. **1**, 202 (1962).
[27] T. Fliessbach, H. J. Mang, and J. O. Rasmussen, Phys. Rev. C **13**, 1318 (1976).
[28] I. Tonozuka and A. Arima, Nucl. Phys. **A323**, 45 (1979).
[29] T. Fliessbach and S. Okabe, Z. Phys. A **320**, 289 (1985).
[30] F. A. Janouch and R. J. Liotta, Phys. Rev. C **27**, 896 (1983).
[31] G. Dodig-Crnkovic, F. A. Janouch, and R. J. Liotta, Phys. Scr. **37**, 523 (1988).
[32] S. M. Lenzi, O. Dragun, E. E. Maqueda, R. J. Liotta, and T. Vertse, Phys. Rev. C **48**, 1463 (1993).
[33] D. S. Delion and J. Suhonen, Phys. Rev. C **61**, 024304 (2000).
[34] A. Insolia, P. Curutchet, R. J. Liotta, and D. S. Delion, Phys. Rev. C **44**, 545 (1991).
[35] D. S. Delion, A. Insolia, and R. J. Liotta, Phys. Rev. C **46**, 884 (1992); **46**, 1346 (1992).
[36] D. S. Delion, A. Insolia, and R. J. Liotta, Phys. Rev. C **49**, 3024 (1994).
[37] D. S. Delion, A. Insolia, and R. J. Liotta, Phys. Rev. C **54**, 292 (1996).
[38] J. O. Rasmussen, Phys. Rev. **113**, 1593 (1959).
[39] Y. A. Akovali, Nucl. Data Sheets **84**, 1 (1998).
[40] D. S. Delion and A. Sandulescu, J. Phys. G **28**, 617 (2002).
[41] K. Varga, R. G. Lovas, and R. J. Liotta, Phys. Rev. Lett. **69**, 37 (1992).
[42] P. Schuck, A. Tohsaki, H. Horiuchi, and G. Röpke, in *The Nuclear Many Body Problem 2001*, edited by W. Nazarewicz and D. Vretenar (Kluwer Academic Publishers, Dordrecht, 2002), p. 271.
[43] P. M. Morse and H. Feshbach, *Methods of Theoretical Physics* (McGraw-Hill, New York, 1953).
[44] D. S. Delion and R. J. Liotta, Phys. Rev. C **58**, 2073 (1998).
[45] J. Dudek, Z. Szymanski, and T. Werner, Phys. Rev. C **23**, 920 (1981).
[46] A. Bohr and B. Mottelson, *Nuclear Structure* (Benjamin, New York, 1975), Vol. 1.
[47] P. Möller, J. R. Nix, W. D. Myers, and W. J. Swiatecki, At. Data Nucl. Data Tables **59**, 185 (1995).
[48] Yu. Ts. Oganessian *et al.*, Phys. Rev. C **62**, 041604 (2000).
[49] S. Hofmann *et al.*, Z. Phys. A **350**, 277 (1995).
[50] S. Hofmann *et al.*, Z. Phys. A **354**, 229 (1996).
[51] Yu. Ts. Oganessian *et al.*, Phys. Rev. Lett. **83**, 3154 (1999).
[52] V. M. Strutinsky, Nucl. Phys. **A95**, 420 (1967); **A122**, 1 (1968).
[53] R. Blendowske, T. Fliessbach, and H. Walliser, Nucl. Phys. **A464**, 75 (1987).